In-depth cerebrospinal fluid quantitative proteome and deglycoproteome analysis; presenting a comprehensive picture of pathways and processes affected by multiple sclerosis

Ann Cathrine Kroksveen[1,2*¤], Astrid Guldbrandsen[1,2¤], Marc Vaudel[1,3,4], Ragnhild Reehorst Lereim[1,2], Harald Barsnes[1,5], Kjell-Morten Myhr[2,6], Øivind Torkildsen[2,6], Frode S. Berven[1,2,6*]

1. Proteomics Unit (PROBE), Department of Biomedicine, University of Bergen, Bergen, Norway.
2. The KG Jebsen Centre for MS-research, Department of Clinical Medicine, University of Bergen, Bergen, Norway.
3. Center for Medical Genetics and Molecular Medicine, Haukeland University Hospital, Bergen, Norway
4. KG Jebsen Center for Diabetes Research, Department of Clinical Science, University of Bergen, Norway
5. Computational Biology Unit, Department of Informatics, University of Bergen, Bergen, Norway.
6. The Norwegian Multiple Sclerosis Competence Centre, Department of Neurology, Haukeland University Hospital, Bergen, Norway.

Keywords: Multiple sclerosis, cerebrospinal fluid, TMT, biomarkers, protein networks, glycosylation, inflammation, immune system, neuron development

¤ Equal contribution
*Corresponding authors
Frode S. Berven, Proteomics Unit, Department of Biomedicine, University of Bergen, Jonas Lies vei 91, N-5009 Bergen, Norway. Telephone: +47 55586378. e-mail: Frode.Berven@uib.no
Ann Cathrine Kroksveen, Proteomics Unit, Department of Biomedicine, University of Bergen, Jonas Lies vei 91, N-5009 Bergen, Norway. Telephone: +47 55586378. e-mail: Ann.Kroksveen@uib.no

ABSTRACT

In the current study, we conducted a quantitative in-depth proteome and deglycoproteome analysis of cerebrospinal fluid (CSF) from relapsing-remitting multiple sclerosis (RRMS) and neurological controls using mass spectrometry and pathway analysis. More than 2000 proteins and 1700 deglycopeptides were quantified, with 484 proteins and 180 deglycopeptides significantly changed between pools of RRMS and pools of controls. Approximately 300 of the significantly changed proteins were assigned to various biological processes, including inflammation, extracellular matrix organization, cell adhesion, immune response and neuron development. Ninety-six significantly changed deglycopeptides mapped to proteins that were not found changed in the global protein study. In addition, four mapped to the proteins oligo-myelin glycoprotein and noelin, which were found oppositely changed in the global study. Both are ligands to the nogo receptor, and the glycosylation of these proteins appears to be affected by RRMS. Our study gives the most extensive overview of the RRMS affected processes observed from the CSF proteome to date, and the list of differential proteins will have great value for selection of biomarker candidates for further verification.

Data are available *via* ProteomeXchange with identifier PXD004572 and PXD004540.

INTRODUCTION

Multiple sclerosis (MS) is an inflammatory disease of the central nervous system (CNS) which causes demyelination and axonal damage. The disease affects more than 2 million people worldwide and is the most common cause of neurological disability in young adults besides trauma [1]. The etiology of MS is still unknown, but data implies that susceptibility to MS is a combination of genetic and environmental risk factors [2, 3].

Currently there is no general cure for MS. Multiple disease modifying drugs are available (reviewed in [4, 5]), but they may be moderately effective and result in serious side effects [6-9]. In the recent years, hematopoietic stem cell transplantation has emerged as a treatment option, but at the moment it is only given to patients with severe and aggressive MS [10, 11]. Novel medication offers new possibilities for individualized treatment, but also raises new questions given that the heterogenic nature of MS may complicate the treatment decisions. It is therefore critical to understand the nature of the disease and how the disease pathogenesis varies between patients. Disease activity and therapeutic efficiency is at present measured through relapse rate, magnetic resonance imaging (MRI) outcome, and changes in the expanded disability status scale (EDSS) score (reviewed in [4]), which all have limited sensitivity. New biomarkers for diagnosis, therapeutic response and disease progression are therefore needed.

Cerebrospinal fluid (CSF) is the most commonly used body fluid for studying neurological disorders as it reflects ongoing pathological and inflammatory processes related to CNS diseases [12]. Normally, the blood-brain-barrier (BBB) protects the CNS from entry of immune cells, but in MS this protective barrier is disrupted, and this allows for activated immune cells to migrate across the BBB. Proteomics has already proven useful for biomarker studies in MS, and elevated chitinase-3-like protein 1 (CHI3L1) levels in CSF was suggested as a biomarker for disease progression from clinically isolated syndrome (CIS) to clinically definite MS (CDMS) [13] as well as a potential biomarker for therapeutic response [14].

A number of biomarker studies have been published for MS (reviewed in [15]), but they all present a low number of quantified proteins compared to the number of identified proteins in CSF [16, 17]. Furthermore, none of these studies provide quantitative information for the glycoproteome, which is expected to contain promising biomarkers for various diseases, including MS [18-21]. In a recent glycoproteome experiment in CSF from neurologically healthy patients, more than 500 glycoproteins from over 1,100 deglycopeptides were identified [16], indicating that the CSF glycoproteome could be an important source of information for monitoring CNS processes.

In this study, we present a quantitative in-depth comparison of CSF from RRMS patients and neurological controls, with protein quantification data for more than 2,000 proteins and 1,700 deglycopeptides. This is the most comprehensive quantitative proteomics study of the CSF proteome to date, and it provides a new and deeper level of information about the pathological processes in RRMS patients reflected in the CSF proteome.

EXPERIMENTAL PROCEDURES

CSF collection and patient information

CSF was collected from individuals that underwent a diagnostic lumbar puncture (LP) at the Department of Neurology, Haukeland University Hospital, Bergen, Norway, according to the recommended consensus protocol for CSF collection and biobanking [22]. All RRMS patients were diagnosed according to the revised McDonald criteria [23] and were diagnosed as RRMS at the time of LP. The samples comprised CSF from 21 patients diagnosed with RRMS and 21 controls with other neurological diseases (OND). The OND controls were evaluated by a neurologist to have no risk of developing MS. None of the RRMS patients received medication prior to the LP. All RRMS patients had oligoclonal CSF bands (OCB), whilst all OND controls were OCB negative. All included CSF samples had to have normal protein concentration and cell count. Detailed patient information is shown in **Table S1**. The study was approved by The Regional Committee for Medical Research Ethics of Western Norway. Written informed consent was obtained from all patients and controls.

Preparation of pooled samples

The 42 CSF samples were randomly divided into three pools of RRMS patients and three pools of OND controls, using controlled randomization ensuring that one male was in each pool, resulting in six pools with seven individuals in each pool (**Table S1** and **Figure 1A**). Equalized CSF amounts presenting 200 µg of protein total content from every donor were used to create the pools, making the final total protein amount in each pool 1,400 µg. The CSF protein concentration was measured using turbidimetry instrumentation (Roche). The total protein concentration in each pool is shown in **Table 1**. The same pools were used for both the global proteome analysis and the glycoproteome analysis.

Table 1. Summary information on all CSF donors.

	Pool 1	Pool 2	Pool 3	Pool 4	Pool 5	Pool 6	t-test *p*-value
Diagnosis	RRMS	RRMS	RRMS	OND	OND	OND	
n	7	7	7	7	7	7	
Male/female	1/6	1/6	1/6	1/6	1/6	1/6	
Age at LP.	36.4 (7.5)	38.3 (6.7)	35.7 (8.3)	34.1 (9.7)	35.7 (9.2)	36.4 (8.6)	0.5798
Total [protein] (µg/µL)	0.314 (0.091)	0.311 (0.157)	0.335 (0.070)	0.326 (0.113)	0.369 (0.095)	0.330 (0.106)	0.6164
[IgG] (µg/µL)	0.069 (0.038)	0.056 (0.035)	0.053 (0.024)	0.026 (0.013)	0.031 (0.012)	0.027 (0.017)	0.0003
# months from first symptom to LP	10.6 (22.2)	11.1 (18.4)	9.4 (10.5)	N/A	N/A	N/A	
EDSS score at LP	1.4 (0.79)	1.2 (0.70)	1.2 (1.07)	N/A	N/A	N/A	
OCB positive	100	100*	100	0	0	0	
Total [protein] after depletion (µg/µL)	0.743	0.839	0.953	1.41	1.01	1.30	0.0419
TMT label global proteome analysis	126	128	130	127	129	131	
TMT label deglycoproteome analysis	128	130	127	126	129	131	

*One patient was not analyzed for OCB (oligoclonal bands). All data are expressed as mean (SD).

Chemical, reagents and solutions

Iodoacetamide (IAA), urea, calcium hydrochloride, methylamine, N-Octyl-β-D-glucopyranoside (NOG), ammonium formate, DTT, sodium periodate and PNGase F enzyme were purchased from Sigma Aldrich. Trypsin was purchased from Promega (sequencing grade). Affi-Prep® Hz hydrazide support slurry was purchased from Bio-Rad (control 210011598). Water, ACN, TFA and formic acid (FA) were purchased from Sigma Aldrich and were mass spectrometry grade. Tandem-mass-tag (TMT) 6-plex reagents were purchased from ThermoFischer Scientific (Lot number OI191932). Solutions for protein depletion were purchased from Agilent Technologies.

Sample preparation, protein depletion, protein digestion and TMT labeling

Global proteome analysis

A CSF aliquot from each pool (500 µg) was immunodepleted (MARS Hu-14, 4.6 mm x 50 mm LC column, Agilent Technologies), desalted and concentrated as described previously [24]. The protein concentration after depletion was measured in each pool using the Qubit™ fluorometer (Invitrogen) and 30 µg protein from each pool were in-solution digested as described in [25], except that trypsin was used in a 1:40 ratio. Each sample was desalted using the reverse phase Oasis® HLB µElution Plate 30 µm (Waters), labeled using TMT 6-plex reagents as detailed in Table 1, combined according to the manufacturer's protocol and desalted as described in [24]. The experimental workflow is illustrated in Figure 1B. The labeling efficiency was investigated prior to combining the TMT labeled samples, and showed an efficiency of > 99%.

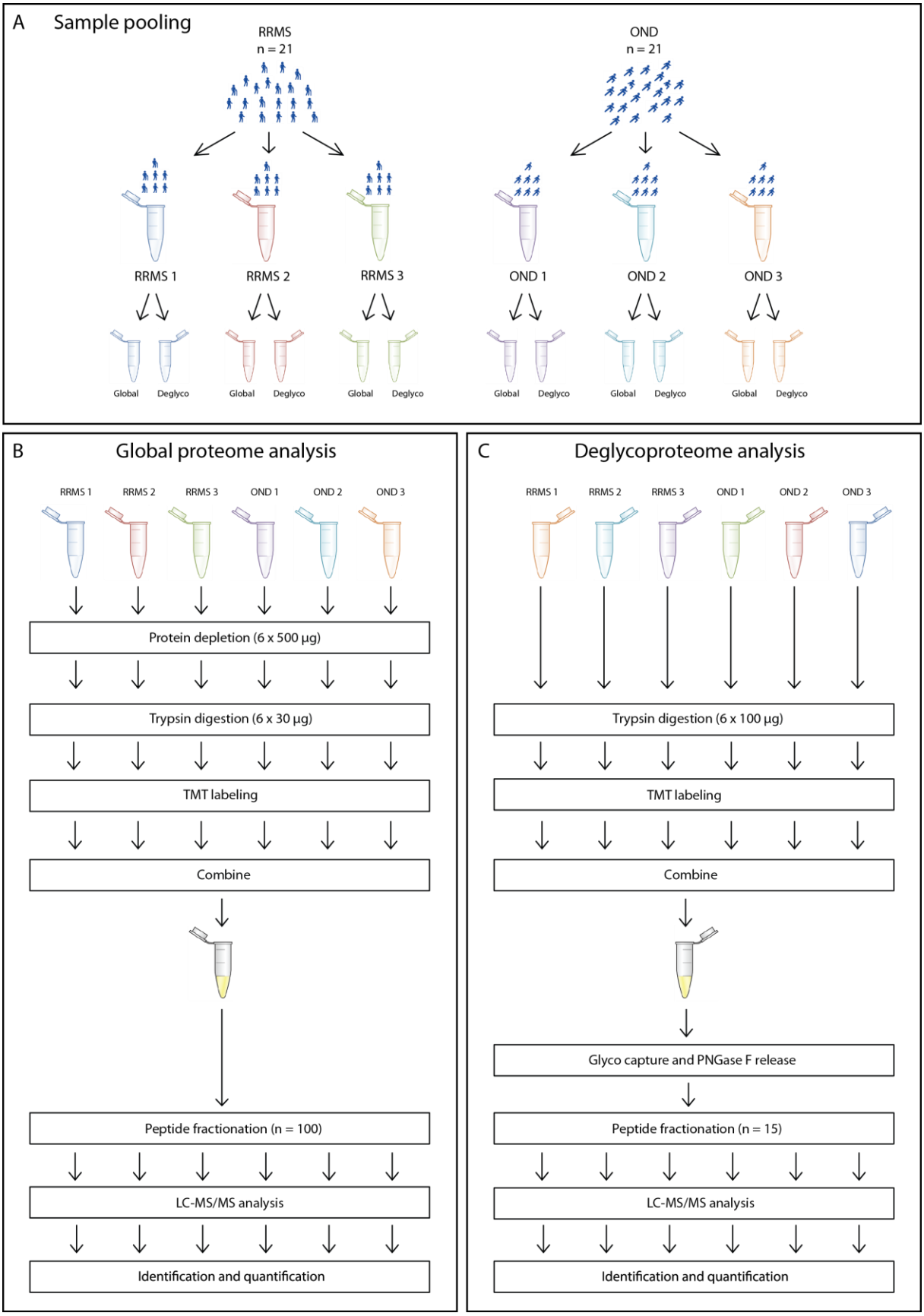

Figure 1. Illustration of the pooling procedure (A) and the workflow of global (B) and deglycoproteome (C) experiments performed in this study. The pooling procedure shown in Figure 1A illustrates that 21 relapsing-remitting multiple sclerosis (RRMS) patients and 21 neurological controls with other neurological

diseases (OND) were separated into six pools, with seven individuals in each pool. These pools were used for two separate experiments: B) Global proteome analysis and C) Deglycoproteome analysis. Only the global experiment included protein depletion (B), while trypsin digestion, TMT labeling and combination of the labeled pools was common for both experiments. Glycopeptide capture by solid-phase enrichment of N-linked glycopeptides (SPEG) was then performed in the glycoproteome experiment (C), followed by peptide fractionation, LC-MS/MS analysis and protein and peptide identification and quantification, which was common for both experiments.

Deglycoproteome analysis

A CSF aliquot from each pool (100 µg) was purified and concentrated using 3 kDa ultracentrifugation filters as described in [26], in-solution trypsin digested, desalted and TMT labeled as described for the global proteome analysis. Approximately 1.5 µg was taken from each sample for testing the labeling efficiency, which was found to be > 99%.

Glycopeptide enrichment

The samples for the deglycoproteome analysis were combined, concentrated and dissolved in 300 µL 0.1% TFA and further acidified by addition of 2 µL 100% TFA before a new Oasis® HLB desalting, now using a 10 mg plate as previously described [26]. The resulting sample was then concentrated, oxidized in 10 mM sodium periodate, 0.1% TFA, and desalted by Oasis® HLB as in [26]. Oasis eluate was added to 50 µL Affi-Prep® Hz hydrazide support slurry, prewashed with 1 mL deionized water. Beads and peptides incubated overnight before beads were washed and deglycosylated peptides were released by PNGase F digestion, desalted by Oasis® HLB µElution and concentrated, as described in [16, 26]. Five percent of the sample was saved for prefractionation LC tandem mass spectrometry analysis, in case some peptides were lost during fractionation. The experimental workflow is illustrated in Figure 1C.

Sample fractionation

The TMT labeled peptides were fractionated (100 fractions for the global proteome analysis and 15 for the deglycoproteome analysis) using mixed-mode chromatography on a Sielc Promix MP column (MP-10.250.0530, 1.0 × 250 mm, 5 µm, 300Å, Sielc Technologies) and an Agilent 1260 series LC system (Agilent Technologies). The peptides were reconstituted in buffer A (20 mM ammonium formate, 3% ACN) and loaded on the column using 15% buffer B (2 mM ammonium formate, 80% ACN, pH 3.0). Details for the gradient and fraction collection are in **Table S2**.

Liquid chromatography mass spectrometry analysis

Each fraction (100 for the global proteome analysis and 15 for the deglycoproteome analysis) as well as the prefractionation deglycoproteome sample was freeze dried in a Centrivap Concentrator (Labconco) and dissolved in 2% ACN, 1% FA. Approximately 0.5 µg of peptides from each fraction was injected into an Ultimate 3000 RSLC system (Thermo Scientific) connected to a Q-Exactive HF equipped with an EASY-spray ion source (Thermo Scientific). The samples were loaded and desalted on a pre-column (Acclaim PepMap 100, 2 cm x 75 µm i.d. nanoViper column, packed with 3 µm C18 beads) at a flow rate of 3 µL/min for 5 min with 0.1% TFA. The peptides were separated during a biphasic ACN gradient from two nanoflow UPLC pumps (flow rate of 0.200 µL/min) on a 50 cm analytical column (PepMap RSLC, 50 cm x 75 µm i.d. EASY-spray column, packed with 2 µm C18 beads (Thermo Scientific). Solvent A was 0.1% FA in water and Solvent B was 100% ACN. The fractions were applied different LC-methods depending on their elution time from the mixed-mode column (**Table S3**). For the deglycoproteome experiment, all fractions were initially analyzed using one LC-gradient. Additionally, since peptides in fractions 7-15 eluted very late in the gradient, those fractions were reanalyzed using a longer (105 min) gradient (**Table S3**).

The mass spectrometer was operated in data-dependent acquisition mode to automatically switch between full scan MS1 and MS2 acquisition. The instrument was controlled through Q Excative HF Tune 2.4 and Xcalibur 3.0. Mass spectrometry spectra were acquired in the scan range 375-1500 *m/z* with resolution 60,000 at *m/z* 200, automatic gain control (AGC) target of 3e6 and a maximum injection time (IT) of 50 ms. The 12 most intense eluting peptides above intensity threshold 6e4, and charge states two or higher, were sequentially isolated for higher energy collision dissociation (HCD) fragmentation and MS2 acquisition to a normalized HCD collision energy of 32%, target AGC value of 1e5, resolution R = 60,000, and IT of 110 ms. The precursor isolation window was set to 1.6 *m/z* with an isolation offset of 0.3 and a dynamic exclusion of 30 seconds. Lock-mass (445.12003 *m/z*) internal calibration was used [27] and isotope exclusion was on.

Data Interpretation

Global proteome analysis

All raw files were converted to mgf using Proteowizard [28] and searched using X!Tandem [29], MyriMatch [30], and Comet [31] *via* SearchGUI (v. 2.8.5) [32] against the *Homo Sapiens* complement of the UniProt/SwissProt reviewed database downloaded April 2016 (20,200 entries) [33]. All non-human contaminant proteins from the Global Proteome Machine cRAP

protein sequences (ftp://ftp.thegpm.org/fasta/cRAP/) were added to the downloaded database as well as a reversed version of every sequence as decoys. The search settings were: carbamidomethylation of C, TMT-6plex labeling on K and N-terminal as fixed modifications; oxidation of M as variable modification; trypsin as enzyme with a maximum of 2 missed cleavages; precursor charge 2-5; peptide length 6-30; precursor and fragment mass tolerance 10 ppm. All other settings were left to default.

The search engine results were combined and assembled in PeptideShaker [34] (v. 1.10.2). Notably, protein ambiguity groups were made to account for the presence of shared peptides between protein sequences [35], and all hits were thresholded to retain only the best scoring until reaching a false discovery rate (FDR) of 1% estimated using the distribution of target and decoy hits [36]. Throughout the manuscript, peptides and proteins refer to peptides and protein groups validated at 1% FDR. The default quality control filters of PeptideShaker were used and the peptides and proteins passing this additional quality control are referred to in the following as confidently identified. The confidence in the localization of posttranslational modifications was evaluated using the D-score [37] and PhosphoRS [38] using the default settings of PeptideShaker.

Peptides and proteins were quantified according to [39] using Reporter (http://compomics.github.io/projects/reporter.html) (v. 0.3.4) and default settings. Briefly, the reporter ion intensities were deisotoped using the purity coefficients provided by the manufacturer. For every peptide, abundance ratios were estimated from the aggregation of spectrum level ratios using all fractions. In every channel, the peptide ratio estimation was done using robust estimators: the median was used if less than six ratios were found, a redescending M-estimator elsewise. Using the median or averages of channels has been demonstrated to be preferable over using one reference pool [40]. Peptide ratios were normalized to the median of those peptides that were derived from the list of brain specific proteins presented by Aasebø *et al.* [24] as suggested as the best way for normalization of CSF quantitative proteomics [41]. Protein group ratios were finally estimated from peptide ratios using the same estimators. For every TMT channel, proteins ratios were normalized to the median of the stable proteins as done for the peptides. All human keratins, proteins targeted by the depletion column, contaminants and proteins that did not have quantitative values in all TMT channels were removed from the dataset (n = 89). The remaining 2,877 proteins were included for statistical analysis after logarithm base two transformation. An F-test was used to investigate equality of variances between the patients and controls, and a Student's t-test with unequal variances was used when the F-test was significant ($p < 0.05$) (n = 174). A Student's

t-test with equal variances was used otherwise. The Benjamini-Hochberg correction was used as multiple hypothesis test. We further calculated a Z-score to identify most prominent fold change (FC) differences between the two groups (RRMS and OND). The FC was calculated based on the difference of averages. Proteins with doubtful validation status were removed, in addition to removing proteins with fewer than two validated and unique peptides. The remaining 2,072 proteins are referred to as quantified. A *p*-value < 0.05 from the t-test was considered as significant, and the 484 statistically significant proteins were included for network analysis and GO-enrichment.

Deglycoproteome analysis

All raw files (n = 25: 15 fractions + 9 re-runs of late eluting fractions + 1 prefractionation sample) were identified and quantified as described above except deamidation of N was added as variable modification. A peptide list containing the normalized ratios was exported from Reporter and further data processing was performed in Excel. Contaminant peptides were removed as well as peptides with no quantitative value in at least one of the TMT channels. Adequate routine quantitative methods for the high throughput analysis of glycopeptides, comprising both the amino acid backbone and the glycan moiety, are currently not available Instead, glycans are usually detached proteolytically after enrichment as detailed above, and the remaining amino acid sequence is used as surrogate to estimate the abundance of the glycopeptide [42]. For this, those identified peptides that present a deamidation at an N-glycosylation sequence motif [N][XPˆ][ST] (where XP^ can be any amino acid except proline) are assumed to be the result of a deglycosylation event.. Deglycopeptides were identified as described in [16] with N-glycopeptide enrichment specificity calculated as $\left(\frac{\#glycopeptides}{\#total\ peptides}\right) x\ 100$. Briefly, a deglycopeptide was defined as a peptide containing a deamidation and the N-glycosylation sequence motif, and where a deamidation was not confidently assigned only to an asparagine outside the motif. Hence, for peptides with the N-glycosylation motif and additional asparagines in the sequence but uncertainty in the localization of the deamidation, it was assumed that the deamidation was at the asparagine in the motif as a result of the activity of the PNGase F enzyme. This is based on our calculated low chance of a non-glycopeptide having both a deamidation and the N-glycosylation motif (calculated to be 0.7%) and the fact that N-glycopeptide enrichment had been performed. Briefly, to get an idea of the false glycosite identification rate, we performed an additional search of the corresponding global data with deamidation of asparagine as a variable

modification. Using this dataset we found that the chances of a deamidation occurring in a peptide containing the N-glycosylation sequence motif was about 0.7%. Deglycopeptides that had at least one deamidation confidently localized on an asparagine in the N-glycosylation motif were termed *high confident* deglycopeptides. Those peptides where the localization was doubtful or random, indicating that the scoring algorithms could not confidently assess the exact position of the deamidation, were termed *medium confident de*glycopeptides, although it is likely that the deamidation is on the asparagine in the motif, because of the enrichment performed. Only 23 of the 2,153 peptides identified in the glycopeptide enrichment experiment included both a deamidation and the N-glycosylation motif, where the deamidation(s) was confidently assigned only to asparagine(s) outside the motif. These peptides were not considered deglycopeptides.

Significant differences in peptide ratios between patients and controls were identified using a Student's t-test as described for the global proteome. Furthermore, significant peptides ($p < 0.05$) were thoroughly investigated to see if other variants of the peptide were also present in the dataset, due to miscleavages or other combinations of modifications on the peptide (oxidized M, deamidation of N, etc.), and if they had similar or opposite regulation (further described in the **Supplemental Information**). Deglycopeptide FC abundance differences were then compared to the global proteome experiment to identify similar and different regulations revealed by the two approaches.

Sharing of data through PRIDE

The mass spectrometry proteomics data have been deposited to the ProteomeXchange Consortium [43] *via* the PRIDE [44] partner repository with the dataset identifier PXD004572 for the global data and PXD004540 for the glycoproteome data.

Protein network analysis

All of the 484 significantly different proteins from the global proteome analysis were imported into STRING [45] with interaction sources being experiments and databases, and the interaction score set to medium confidence. The three proteins Ig kappa chain C region, semaphorin-3B, and neurofilament light polypeptide (NFL) were not imported as STRING could not "detect any proteins by the name in Homo sapiens". The STRING network was exported to Cytoscape v.3.3.0 [46]. The Cytoscape plugins BINGO [47] ClusterONE [48] were used for visualization of the STRING network and cluster analysis. In the cluster analysis, a minimum of five proteins was used for network size and interaction evidence towards the

combined score from STRING. All other settings were left to default. The Cytoscape plugins ClueGo [49] and CluePedia [50] were used for Gene Ontology (GO) analysis of biological processes (Homo sapiens GO updated 14.06.16). GO-term fusion and "show pathways with *p*-value < 0.05" were activated. Evidence was set to "All without inferred from electronic annotation (IEA)" and the network specificity was medium. In the ClueGO analysis, all proteins significantly increased in the RRMS patients were analyzed as one group (named Cluster 1 by ClueGO) and the proteins significantly decreased in the RRMS patients were analyzed as a second group (named Cluster 2 by ClueGO). These two clusters were compared by ClueGO, and resulted in two pie charts of biological processes. One pie chart showed the enrichment of genes increased in RRMS (Cluster 1) and the other pie chart showed the enrichment of genes decreased in RRMS (Cluster 2). A corresponding GO term table was also generated presenting the genes behind each term. All other settings were left to default. GO analysis with ClueGO and CluePedia was also done for the glycoproteome using similar settings.

Comparing significant proteins against relevant literature data

In order to compare our protein quantification data against relevant and comparable literature, we thoroughly investigated previously published quantitative CSF proteome datasets presenting biomarkers for MS, Parkinson's disease (PD) and Alzheimer's disease (AD) [13, 14, 25, 41, 51-63]. These data were included in an extended version (unpublished) of CSF-PR [16] which was used for the comparison. Detailed inclusion criteria for these 17 publications are available in the **Supplemental Information**. To further compare in more detail our 484 significantly changed proteins, we extracted quantitative data from those studies comparing RRMS, CIS with conversion to MS or CDMS (collectively called MS) to OND, symptomatic controls or non-MS (collectively called Non-MS). These particular disease groups were chosen because they were similar to the RRMS and control groups used in our study. Eight of the 17 publications included such comparisons [13, 25, 41, 51, 53-56]. Details on the categorization of the literature protein data are available in the **Supplemental Information.**

RESULTS

In this study, pooled CSF was used to analyze the global proteome and deglycoproteome from RRMS patients and controls (n = 21 pooled in three RRMS and 3 control pools) as illustrated in **Figure 1A**. We identified 2,966 and quantified 2,072 proteins in the global proteome

analysis (**Table S4**) and in the deglycoproteome analysis 1,744 deglycopeptides mapping to 697 proteins groups were quantified (**Table S5, C**). STRING [45] analysis and the Cytoscape [46] plugin ClusterONE [48] was used for cluster analysis, while the Cytoscape plugins ClueGO [49] and CluePedia [50] were used for GO-enrichment analysis, as described in the Experimental Procedures.

Global proteome analysis

In the global proteome analysis, we quantified 2,072 proteins with ≥ 2 validated and unique peptides. A Student's t-test was used for statistical analysis and revealed 484 proteins with a *p*-value < 0.05 between the RRMS patients and the controls of which 243 were increased and 241 were decreased in the RRMS patients (**Table S6, A**). The 2,072 quantified proteins were compared to 17 previously published studies as explained in the materials and methods, and quantitative information had not been reported for 1,273 of them. Of the 484 significantly changed proteins 236 (49%) had not been quantified in any of the 17 studies, whereas 248 (51%) had.

We further compared the 484 significantly changed proteins to the regulations of these proteins found in eight other studies analyzing patient groups similar to ours [13, 25, 41, 51, 53-56]. Of the 248 proteins found in all 17 studies, 216 were quantified in these eight studies and we divided the 216 hits into five categories based on their correlation with the literature data. More information about this categorization is in **Supplemental Information**. As can be seen from **Figure 2**, 10 of the proteins significantly increased in MS were also reported with increased abundance in the eight comparable studies (Increased 100%). Seventeen proteins fell into the "Increased < 100%" category, indicating that these proteins were found significantly increased in MS in the majority (average) of the studies. The numbers for the proteins significantly decreased in MS were 10 (Decreased 100%) and 50 (Decreased < 100%). For the remaining proteins (129), their abundance had been reported with either opposite significant change (9 proteins) or an average non-significant change (Equal, 120 proteins).

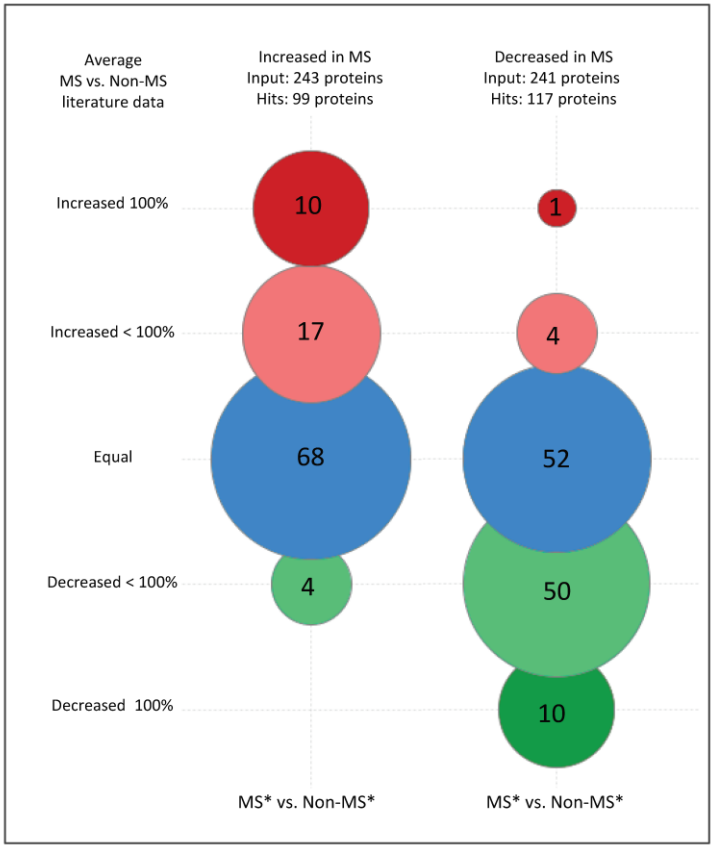

Figure 2: Distribution of protein data for proteins previously quantified in comparable CSF studies. Proteins found significantly increased (left) or decreased (right) in RRMS were compared separately to eight publications. Red circles represent the query proteins found increased in MS compared to Non-MS in 100% of the studies and pink circles represent the proteins found increased in MS in the majority of studies, but with some conflicting data. Green and light green circles represent these same trends for the decreased proteins. The blue circles represent the proteins found unaltered between MS and Non-MS on average in the seven studies. The MS category is a combination of the reported MS subcategories: RRMS, CDMS and CIS with conversion to MS, and the Non-MS category is a combination of the control group subcategories reported as OND, Symptomatic controls and Non-MS. More information about this categorization is in **Supplemental Information**. *Combined categories

Deglycoproteome analysis

Glycopeptide identification and quantification

In total 2,153 peptides mapping to 734 protein groups were quantified from the glycopeptide enrichment experiment (**Table S5, B**) of which 1,744 (**Table S5, C**) were identified as deglycopeptides (Experimental Procedures) mapping to 697 glycoproteins. This gave a peptide enrichment specificity of 81%. Of these, 1617 were *high confident deglycopeptides* (**Table S5, D**) and 127 medium confident (data not shown). Furthermore, 153 (< 10%) of the deglycopeptide sequences were also identified in the global peptide dataset, when comparing

against 32,701 confidently validated peptides quantified in all six pools (**Table S5, H**). This shows that both a glycosylated and non-glycosylated form of these proteins is likely to exist.

We retrieved Uniprot glycosylation annotation data for all the proteins to which our glycopeptides mapped and checked our identified sites (only sites on unique peptides and where there was only one possible glycosylation site) against all known sites for these proteins. Information about referenced glycosylation status on both protein and site level can be found in **Table S5, sheet C**. In summary, we identified a total of 1,239 unambiguous glycosylation sites, of which 515 were already referenced in Uniprot and 724 were new. In addition, sites on 62 peptides were termed ambiguous either because they were on non-unique peptides or because there were two possible glycosylation sites. Previously undocumented glycosylation data is here demonstrated (indirectly as deglycopeptides) for 304 proteins.

Categorization of significant deglycopeptides

Of the quantified deglycopeptides, 235 were found to have significant differences between MS and OND (**Table S5, E**). These were manually inspected to reveal if other peptide variants containing the same glycosylation site had conflicting relative abundances in the deglycoproteome dataset. Different peptide variants containing the same glycosylation site could be non-tryptic peptides or appear due to missed cleavages and/or modifications (see **Supplemental Information** for details). This manual validation resulted in 180 non-conflicting significantly changed deglycopeptides (**Table S5, G**) which were used as input for GO enrichment analysis in Cytoscape. Furthermore, 49 of these deglycopeptides also had a significant z-score based on the observed FC (**Table S7)**, and represent the deglycopeptides most likely to be changed in RRMS compared to controls.

Global versus deglycoproteomics experiments

We further compared the deglycopeptide and the global protein FC (log2) for the 180 non-conflicting deglycopeptides (**Table S8, B**). Four deglycopeptides substantially deviated from their protein FC with significant opposite regulation. These peptides derive from oligo-myelin glycoprotein (OMgp) (three peptides, negative FC) and noelin (one peptide, positive FC). OMgp was found significantly increased ($p < 0.01$) in RRMS patients in the global study by 22 peptides, whereas in the deglycoproteome study, all three quantified deglycopeptides were found significantly decreased ($p < 0.05$). Noelin, on the other hand, was significantly decreased ($p < 0.005$) in the global data, but was found with a significantly increased ($p < 0.05$) peptide in the deglycoproteome study. More details on these data are available in **Table**

S8, A, B. We also plotted the FC difference between all 1,744 quantified deglycopeptides and all quantified global proteins, and it was clear that most deglycopeptides display a FC similar to the protein FC from the global experiment (**Table S8, C, D**).

To assess the possibility of identifying glycoproteins in CSF without glyco enrichment procedures, we investigated the known glycosylation status of the 2,072 proteins quantified in the global CSF study, and found that 580 of these were annotated with one or more referenced glycosylation sites in Uniprot. We further compared these to the proteins to which our quantified deglycopeptides mapped. We found that 249 of them were not found in the deglycoproteome experiment, meaning that these proteins could only be identified using the global proteome approach. Information about which proteins have referenced Uniprot glycosylation status and whether they were also found in the deglycoproteome experiment can be found in **Table S4, B.**

GO enrichment analysis of significantly changed proteins and glycoproteins

The Cytoscape plugins ClueGO [49] and CluePedia [50] were used for GO enrichment analysis for comparing which biological processes that were enriched in the RRMS patients, as described in the Experimental Procedures. For the global data, the 484 significant proteins (mapping to 319 unique genes in ClueGO, **Table S9**) were imported, while the 180 non-conflicting significantly changed deglycopeptides (mapping to 138 proteins and 85 unique genes in ClueGO, **Table S5, G** and **Table S10**) were imported for the glycoproteome analysis. The processes that were enriched in proteins significantly increased in RRMS patients are illustrated in **Figure 3 A and B**, and the processes enriched in proteins significantly decreased in RRMS patients are illustrated in **Figure 3 C and D.** Each pie chart is divided into different groups, named according to the leading term for each group. The group leading term was chosen by ClueGO and depends on *e.g.* the number of genes, percentages of found genes and the *p*-value for the different terms. All data for **Figure 3 A and C** (global proteome) can be found in **Table S9** and data for **Figure 3 B and D** (glycoproteome) are found in **Table S10**.

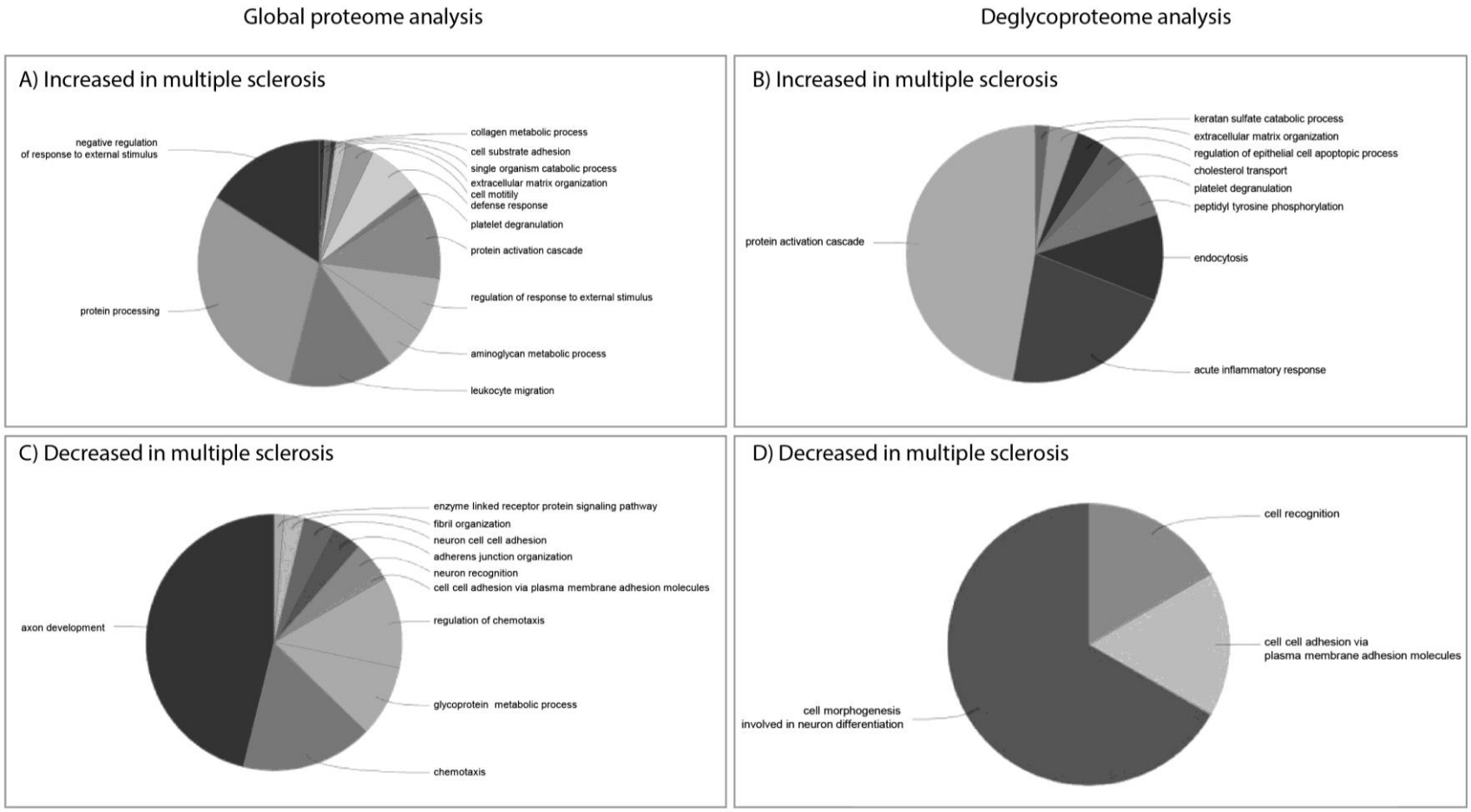

Figure 3. Biological processes GO enriched in proteins increased (A and B) and decreased (C and D) in CSF of RRMS patients. The global data is shown in A (increased in RRMS) and C (decreased in RRMS) and the glycoproteome data is shown in B (increased in RRMS) and D (decreased in RRMS).

As shown in **Figure 3 A and B**, the processes enriched in proteins increased in RRMS patients relate to the inflammatory response, such as protein processing, protein activation cascade, leukocyte migration, acute inflammatory response and defense response. Further, the enriched processes included proteins involved in extracellular matrix (ECM) organization, aminoglycan and chitin metabolic processes, and coagulation. Of the processes that were enriched in proteins decreased in RRMS patients (**Figure 3, C and D**) we found neuron development, including axonal development and cell morphogenesis involved in neuron differentiation, fibril-organization, and chemotaxis.

Global proteome interaction analysis of significantly different proteins

The 484 significantly changed proteins (**Table S6**) were imported into STRING [45] and interactions were found between 222 of the imported proteins. The protein-protein interaction (PPI) network was further exported to Cytoscape [46] and the main network (170 genes) is visualized in **Figure 4**. The two proteins amyloid-beta A4 protein (APP) and epidermal growth factor receptor (EGFR) represented the key nodes (genes) with the highest number of interactions in the PPI network. The EGFR pathway has been indicated to contribute to the inflammation amplifier [64]. Other studies have indicated that inhibition of EGFR protects neurons from degradation and is neuroprotective in rat models of both spinal cord injury [65] and glaucoma [66]. For APP, a wide range of functions have been suggested in the CNS [67], but it is mostly known to be a precursor protein for amyloid beta known to be involved in AD [68].

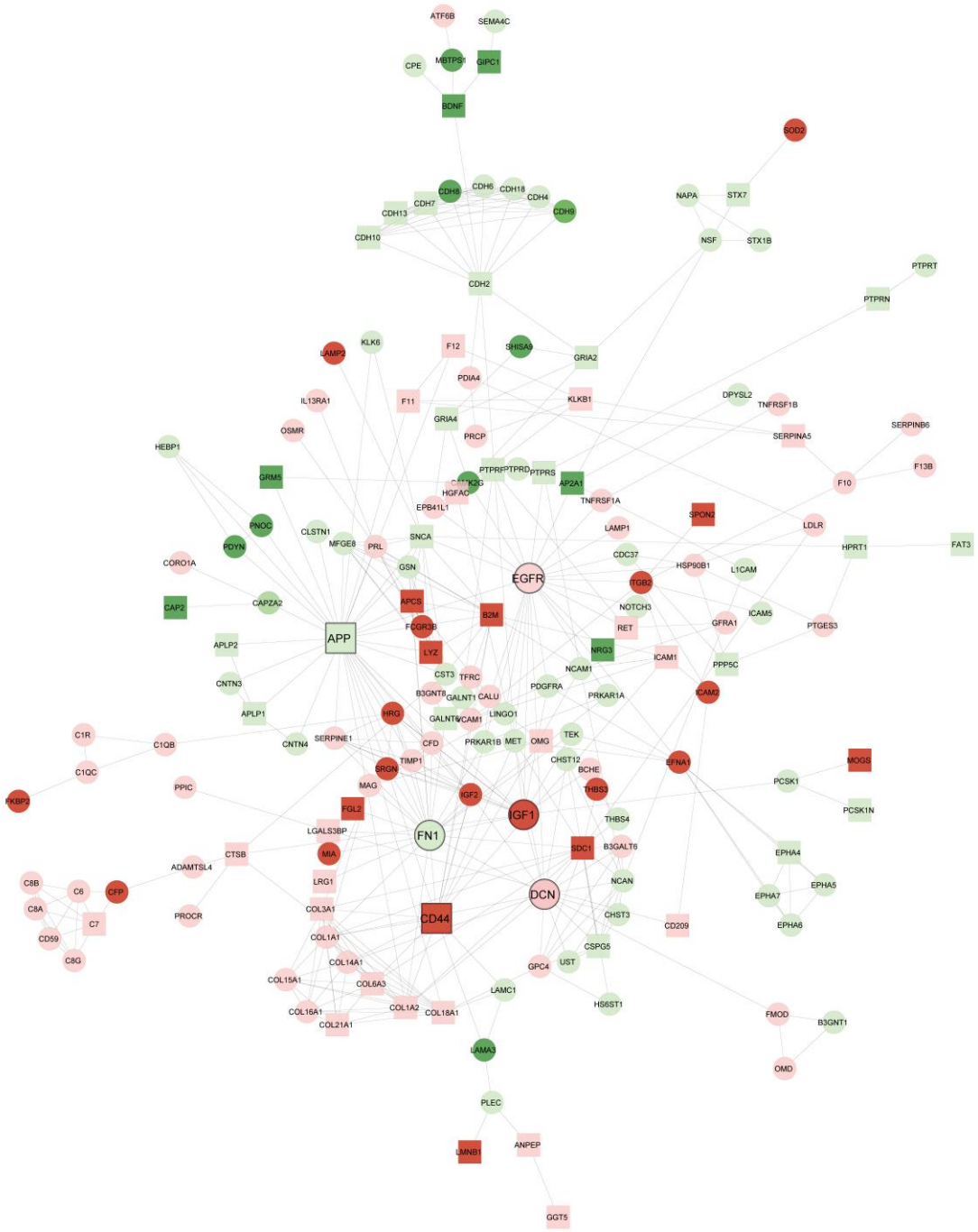

Figure 4. Protein-protein interaction (PPI) network. 484 significantly changed proteins between the RRMS patients and the controls (Table S6) were imported into STRING [45] and interactions were found between 222 of the 484 proteins. The PPI was visualized in Cytoscape v3.3.0. Green and red colors represent lower and higher expression of proteins in CSF between RRMS patients and controls, respectively. Light green and light red represent proteins with z-score significance > 0.05, while the dark green and red proteins have z-score significance < 0.05. Rectangles are proteins with a t-test *p*-value < 0.01, while the proteins represented by a circle have *p*-value between 0.01 and 0.05.

The Cytoscape plugin ClusterONE reported 14 clusters with a *p*-value < 0.05 (**Figure S1**) using the PPI network from **Figure 4** as input. A selection of the most significant clusters containing five or more genes is shown in **Figure 5A-F**. These clusters contain (a) cadherins, involved in cell adhesion, (b) collagens, which are ECM proteins, (c) complement factors, involved in inflammation, (d) ephrins and other proteins involved in synaptic plasticity, (e) proteins involved in aminoglycan processes, and (f) proteins involved in coagulation and inflammation.

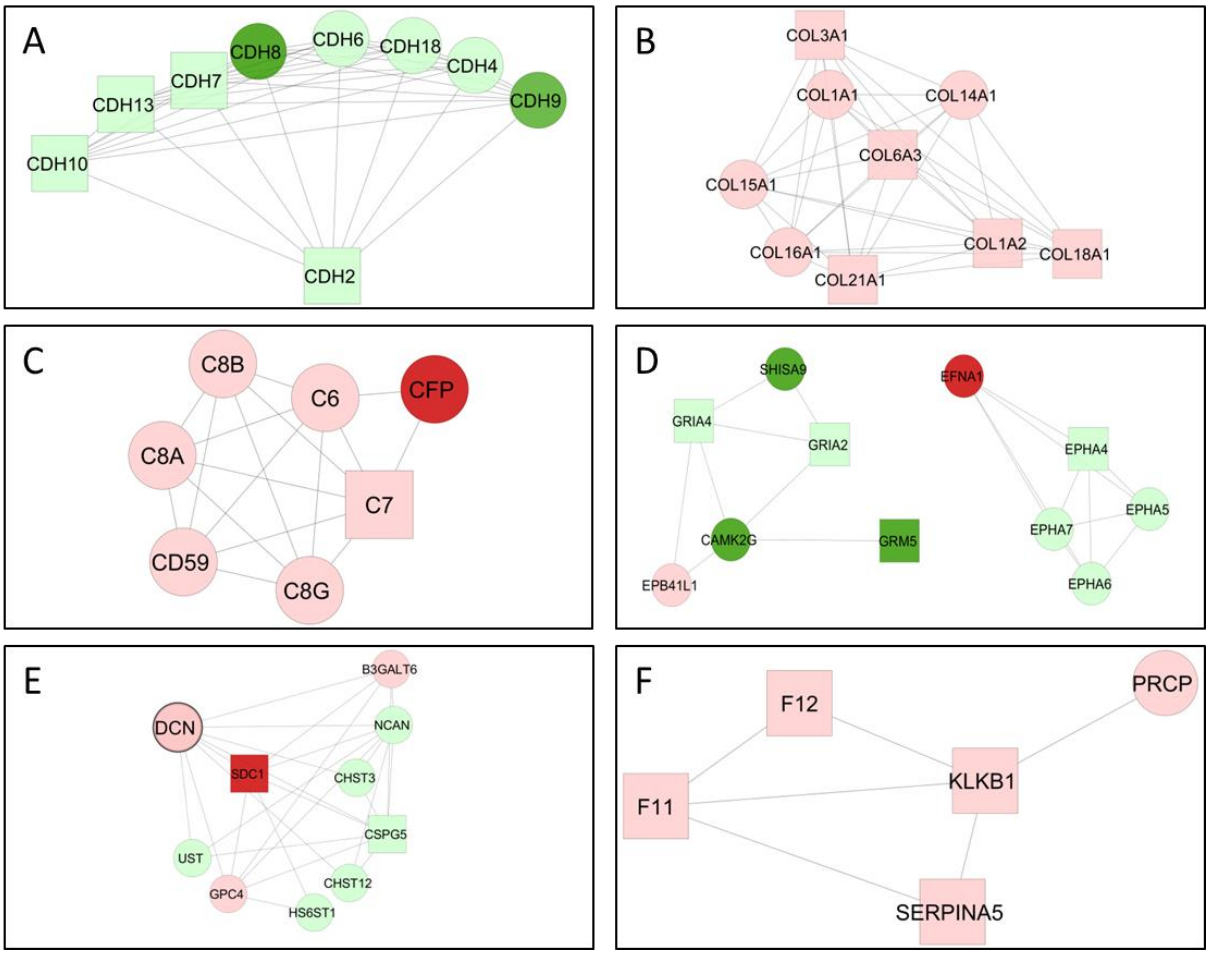

Figure 5. Cluster analysis of the protein-protein interaction network using ClusterONE. A minimum of five genes was included in the network and interaction evidence towards the combined score from STRING. a) cadherins b) collagens c) complement proteins d) ephrins and proteins involved in synaptic plasticity e) proteins involved in aminoglycan processes f) proteins involved in the coagulation and inflammation. Green and red colors represent lower and higher expression of proteins in CSF between RRMS patients and controls, respectively. Light green and light red represent proteins with z-score significance > 0.05, while the dark green and red proteins have z-score significance < 0.05. Rectangles are proteins with a t-test *p*-value < 0.01 while the proteins represented by a circle have *p*-value between 0.01 and 0.05.

DISCUSSION

In the present study, we compared the CSF global and glycoproteome between RRMS patients and controls using TMT-labeling, extensive peptide fractionation, and state of the art bioinformatics. More than 2,000 proteins and 1,700 deglycopeptides were identified and relatively quantified with high confidence, and we hereby present the most comprehensive quantitative CSF proteomics study to date.

The pooling strategy undertaken in our study allows us go deep into the CSF proteome to reveal novel information about how RRMS affects the CSF proteome. When pooling samples, information about biological variation between individuals is lost, but other studies have shown no systematic bias due to pooling [69] as well as agreement between the protein expression in pools and the mean of individual samples [70]. This is in accordance with our own observations when comparing our pooling data to previously published work and we therefore conclude that the observed protein regulations in general are in concordance with the mean measurements of the individuals. Based on this the pooling strategy was considered as a suitable approach particularly since our study is focused on the processes affected by MS at large and not on finding single biomarker candidates.

Our study provides additional evidence for differential expression of previously discovered biomarker candidates, in addition to novel findings. The fact that 236 of the 484 proteins found as significantly changed have not been quantified in any of the 17 recent publications we compared our data to shows that our data revealed regulations occurring in a deeper part of the proteome not previously studied. CHI3L1, CHI3L2 and NFL are among the few proposed biomarkers that have previously been confirmed to be affected by MS [13, 53, 71-73]. We found these proteins significantly changed in agreement with the literature, demonstrating how CSF quantitative proteomics can reliably and reproducibly detect significant changes associated with neurological disorders. In addition, 87 of our significantly different proteins have previously been found with similar regulation in other studies (Figure 2). This shows that the pooling strategy used here provides reliable quantitative information.

Since LP is an invasive procedure, it is important to investigate the possibility to observe significant CSF changes also in serum or plasma. This has been done in some studies [13, 53, 54, 74], attempting to verify biomarker candidates found in CSF. Some of the most studied proteins in CSF and serum are CHI3L1, CHI3L2 and NFL [13, 53, 74, 75]. Significant increase of CHI3L1 have been found in serum of CIS and RRMS patients compared to non-inflammatory neurological controls [53], but increased CSF CHI3L2 levels found in RRMS compared to CIS and non-inflammatory neurological controls were not confirmed in serum [53]. Others have also

investigated the effect of treatment on CHI3L1, and a trend towards decrease in the plasma CHI3L1 levels after treatment with INFβ has been observed [74]. This shows that the CHI3L1 levels between CSF and plasma/serum correlate, but the CHI3L2 levels do not. This offers new possibilities for easier diagnosis and estimation of disease progression and treatment effect. Studies have also investigated other candidate proteins in serum of MS patients [13, 54], but these have found no change between MS subtypes and controls.

To investigate the chance of sampling our 484 significantly changed proteins in blood, we compared them to CSF-PR [16] and the Plasma Proteome Database [76]. We found that 80% of our significantly changed proteins were previously found in plasma or serum, and the remaining proteins were not found (**Table S6**), indicating that they are likely difficult to measure in a blood sample. The list of changed proteins will be a valuable source for selecting new biomarker candidates for MS for further validation. In addition, the deep coverage of the CSF proteome gave us a unique possibility to obtain a broader overview of the RRMS affected processes that can be monitored *via* the CSF proteome.

Cluster analysis and GO enrichment

Inflammation and the immune system

MS is known as an inflammatory disease, and the increase of proteins and pathways related to the immune- and complement system in RRMS are therefore not surprising. A characteristic of the MS brain is the presence of lesions or plaques infiltrated by immune cells, such as T-cells and macrophages [77] which are cells involved in both the innate (native) and adaptive (acquired) immune system. The innate immune system acts in a non-specific manner and has no memory. Contrary, the adaptive immune system has specificity against certain molecules and among others includes CD4+ T-helper cells and CD8+ cytotoxic T-cells (reviewed in [78]).

The BBB normally protects the CNS from entry of immune cells, but in MS this protective barrier is disrupted, allowing for activated immune cells to migrate across the BBB (reviewed in [79]). Why this disruption occurs and how the immune cells enter the CNS is not fully understood, but can hold the key for novel MS treatment. The cells from the innate and adaptive immune system has the ability to produce chemokines, cytokines and other inflammatory factors, which will continue to recruit immune cells into the CNS during the inflammatory event. In accordance with theory, we see an enrichment of proteins significantly increased in RRMS in the GO term leukocyte migration. We do however also see an enrichment of proteins significantly decreased in RRMS in the GO terms chemotaxis and regulation of chemotaxis. Chemokines have the ability to influence the movement of immune

cells by chemotaxis, attracting them towards a higher concentration of chemokines [80]. Our data may imply that the response to such chemical stimuli is impaired in the RRMS patients. This could perhaps be a result of blockage of chemokine receptors on the immune cells, resulting in disturbance of leukocyte movement.

Increased activity of the adaptive immune system, characterized by release of immunoglobulins (Igs), more known as antibodies, is already a well-established trait in RRMS. In our data, we found multiple Ig deglycopeptides increased in the RRMS patients. However, Igs of the adaptive immune system were not found in the global data, due to the removal of IgG, IgM and IgA using protein depletion. We further found increase of the complement proteins C6-C8 (**Figure 5C**), members of the innate immune system that are involved in the generation of the membrane attack complex. Three proteins belonging to the C1-complex, part of the classical complement pathway, were also found increased in these data (**Figure 4**). It has previously been suggested that antibody and complement mediated phagocytosis is involved in the demyelination seen in MS [81].

Furthermore, our GO analysis showed enrichment of proteins increased in RRMS related to the coagulation cascade in MS. This was also seen in the cluster analysis (**Figure 5F**), and has also been found by others [82, 83]. In a study investigating pathways for MS subtypes, the complement and coagulation cascades were demonstrated as a shared pathway for all MS subtypes [82]. In addition, Han *et al.* profiled the MS lesion specific proteome and uniquely identified several coagulation proteins in chronic active plaques, suggesting a dysregulation of molecules associated with coagulation in MS [83]. In the same study, coagulation cascade inhibitors were demonstrated to suppress Th1 and Th17 cytokines in astrocytes and immune cells and to decrease disease severity in an experimental autoimmune encephalomyelitis model. This point towards a role for coagulation cascade participants as potential therapeutic targets [83]. The coagulation proteins we find as increased in CSF could very well appear due to these MS-related CNS processes. The GO analysis also showed an enrichment of proteins increased in platelet degranulation. Platelets have been found to be activated in MS [84] and they are known to alert the immune system during a coagulation process. They may therefore have important roles in the regulation of the innate and adaptive immune processes seen in MS, as they also secrete pro-inflammatory molecules [85, 86].

Extracellular matrix organization

ECM organization was also found as a biological process enriched in RRMS from the GO analysis, and this is also supported by the cluster analysis demonstrating an increase of

collagens. Collagens are important fibrous ECM proteins [87] and mainly appear in the ECM as fibrillar proteins to form various connective tissues [88]. We also see that deglycopeptides from ECM proteins such as fibronectin domain containing proteins, vitronectin and thrombospondin, demonstrate a significant change in RRMS compared to controls. In the brain, ECM proteins not only provide support and structure, but can also have various roles in the development and maturation of neurons [89]. The growth and elongation of many neurons is directed through the ECM and it is therefore not surprising that ECM structures and interactions can influence developing neurons [90]. ECM signaling and recognition are also important in the migration of leukocytes into inflammatory sites and their entry through blood vessels [91]. It has been suggested that the BBB breakdown occurring in MS causes ECM alterations and that deposition of ECM components in active lesions can contribute to disease progression [92]. ECM proteins such as fibrillar collagens have previously been found upregulated in both active and inactive MS lesions [89], and altered expression of collagen has been found in internal jugular veins of MS patients, supporting a role of a vascular involvement in MS [93].

Other ECM proteins highlighted in our cluster (**Figure 5E**) and GO analyses (aminoglycan metabolic processes) (**Figure 3**) are the proteoglycans (PGs), which are macromolecules of the ECM and cell surface. The PGs in our data bears either heparan sulfate or chondroitin [94] and appears in cluster with sulfotransferases. Although PGs are known to have a role in relation to astroglial scarring and axon regrowth after injury [95, 96], few studies have discussed PGs specifically in relation to MS. However, Sobel and colleagues investigated active MS lesions and conclude that white matter ECM PG changes in MS happens in the early inflammatory phases and contribute to failed axonal regrowth and repair [97]. From our analysis it seems clear that alterations in heparan sulfate, chondroitin, and chondroitin sulfate PGs are occurring in RRMS, and we hypothesize that this could be related to the transfer of sulfo groups, based on the many sulfotransferases that interact with the PGs, as shown in **Figure 5E**. The aminoglycan processes also include proteins related to chitin catabolic processes (**Table S9**). CHI3L1 and CHI3L2, chitinase domain-containing protein 1, chitotriosidase-1 and Di-N-acetylchitobiase were found increased in the RRMS patients. Of these proteins, CHI3L1 and 2 lack chitinase activity and have been widely studied in relation to MS over the latest years [13, 14, 51-53].

Neuron development

We found an enrichment of proteins significantly decreased in RRMS in the GO terms axon development, neuron cell-cell adhesion, neuron recognition, and cell morphogenesis involved in neuron differentiation (**Figure 3C** and **D**, **Table S9,** cluster 2 and **Table S10**, cluster 2**).** These categories indicate an impaired development and morphogenesis of neurons, especially with respect to axon development. Neurodegeneration and axonal damage are proposed to be primary mechanisms behind permanent disability in MS [98], and our data support the presence of such processes. Cerebral axonal damage has been demonstrated in early stages of MS, and transected axons, neurons, and apoptotic neurons have been found in MS lesions [99, 100]. In general, the observation of reduced levels of proteins related to neuron development is likely due to an impaired ability in MS patients for neuronal repair after inflammatory damage, or simply a reduced ability to obtain a normal maintenance/turnover of neuronal cells. It would be highly relevant to investigate further the proteins represented in the GO terms mentioned above, to evaluate their potential as therapeutic targets to reduce neurodegeneration in MS, as the current treatment is so far mainly targeting the inflammatory aspect of the disease. A study has shown that the CSF levels of the axonal marker NFL is reduced due to natalizumab treatment, and may have an impact to reduce axonal loss [101]. However, treatment with natalizumab may also have serious side effects. Our supplied list of gene names linked to various GO terms (**Table S9**), *e.g.* those under the GO terms related to neuron development, can provide useful background data to guide future studies investigating new potential treatments targeting neurodegeneration.

Many of the proteins found related to neuron development are ephrin and ephrin receptor proteins which are also highlighted in the cluster analysis (**Figure 5D)**. Ephrin proteins are ligands for the ephrin transmembrane tyrosine kinase receptors and this ligand-receptor signaling has already been linked to the regulation of axonal guidance through the regulation of growth cones [100] and to myelination, as mediators of the signaling between axons and oligodendrocytes [102]. It seems that this signaling can either stimulate or repulse axon growth, and the ephrins may well also be therapeutic targets in MS [103].

Among the 165 proteins not mapped to a gene during the GO analysis (**Table S6**), we find multiple proteins with a potential role in the nervous system. Some of these proteins showed significant interactions in the cluster analysis (**Figure 3D**), and are among other things involved in glutamate signaling, synaptic transmission and synaptic plasticity [104].

Adhesion molecules

Several adhesion molecules were also found decreased in RRMS patients compared to controls in both the global and deglycopeptide datasets, such as the cadherins (**Figure 5A**) and several protocadherin deglycopeptides. Cadherins are transmembrane glycoproteins known for their role in cell adhesion, especially in tissues, where they help maintain a multicellular structure [105]. N-cadherin has previously been linked to de- and remyelination using mouse models [106, 107]. They are further involved in the recruitment and migration of neural progenitor cells into MS lesions and are a key element in promoting repair [106]. Other cell adhesion molecules, including neurexins, neuroligin, integrins and immunoglobulin superfamily molecules, have been found significantly changed in our study, highlighting a possible role of these proteins in MS. A gene pathway study from 2014 links cellular adhesion molecules to MS susceptibility and point to their role in T-cell BBB crossing, which is an important event in the MS pathology [108, 109]. It may well be that the decrease in adhesion molecules are, in fact, also directly linked to the neurodegeneration seen in MS, as their important role in organization and maintenance of tissue structure could be disturbed in affected individuals. **Figure 3C** specifically highlight proteins under the GO terms neuron cell-cell adhesion as decreased in RRMS, supporting this theory. These decreased proteins could therefore also be relevant to investigate further with the aim of targeting the neurodegenerative manifestation of MS.

Cerebrospinal fluid glycosylation data

In comparison with the existing literature on glycopeptides and proteins in CSF, we have by far identified and quantified the highest number of glycopeptides or deglycopeptides to date. In 2006, Pan et al. identified 216 O- and N-linked glycoproteins by a combination of lectin affinity and hydrazide chemistry in addition to 103 non annotated proteins (glycosylation not annotated or protein not in Pubmed) [110]. Furthermore, other studies of glycosylation in CSF include a study by Nilsson et al. from 2009 identifying 36 N-linked and 44 O-linked glycosylation sites in CSF [111], one by Halim et al. from 2012 reporting 84 O-linked intact glycopeptides [112] and one from Goyallon *et al*. from 2015 reporting 124 intact glycopeptides, covering 55 glycosylation sites in 36 proteins [113]. However, the previously most comprehensive characterization of glycosylation in CSF was published by our group in 2014, where we reported 1121 previously glycosylated peptides after PNGase F treatment, and they mapped to 520 proteins [16]. In comparison with referenced glycosylation data in Uniprot, our new data here indirectly demonstrates glycosylation sites for 304 proteins previously not

annotated as glycosylated, however it should be stressed that this data should be further verified by direct identification of the intact glycopeptide.

Our assessment of the Uniprot glycosylation status of all quantified proteins in the global experiment revealed that 580 of these were referenced glycoproteins, and furthermore that 249 of these were not found by our glycopeptide enrichment approach (**Table S4, B**). Since this global experiment gives no information about glycosylation status it may well be that these proteins are simply not glycosylated in CSF, although found glycosylated in other tissues or body fluids (Uniprot). Other reasons for not identifying them in our deglycoproteome experiment might be that they mainly contained O-linked glycosylation sites, which were not targeted by our approach, or that the specific glycosylated peptides also contained additional modifications not considered in our search settings. Finally, the reason may also be that we did not reach the same depth in the deglycoproteome experiment as in the global (depletion and 100 fractions in global vs. no depletion and 15 fractions in glyco).

Comparing significant deglycopeptides to the global proteome data

Many of the significant deglycopeptides demonstrated the same significant changes as their corresponding global protein (**Table S5**, **G)**. However, 96 significantly changed deglycopeptides without corresponding global change were also found (**Table S5**, **G)**. These are likely to come from CSF proteins that are present in both glycosylated and non-glycosylated form, where only the glycosylated form is affected by the disease. They represent an interesting set of potential disease altered glycoproteins, where changes might be associated with glycosylation events.

The same is true for the even more interesting four deglycopeptides with opposite significant changes compared to the global protein. In these cases, MS might have affected the two protein forms differently. These four deglycopeptides mapped to the proteins OMgp (3 peptides), and Noelin (1 peptide). OMgp is a CNS localized membrane glycoprotein ligand for the Nogo receptor, a so-called myelin-associated inhibitor (reviewed in [114]). It has been demonstrated to be an important negative regulator for neurite growth [115, 116]. Noelin is a secreted glycoprotein expressed in neurogenic tissues during development and interestingly, it has also been linked to the Nogo receptor through a study launching Noelin as a ligand for the Nogo A receptor 1 [117]. The Nogo receptor is known to limit the recovery from neural injury and neural plasticity as is reviewed in [118]. Our deglycopeptide regulation data therefore suggest a shift in glycosylation status in RRMS patients of these two proteins that both serve as ligands to the Nogo receptor. It would be interesting to further explore how this affects the

Nogo receptor and possibly neuron growth and myelination, important CNS processes known to be affected in MS.

To validate our glycosylation data and further investigate if glycosylation status is in fact altered in the RRMS pathology, we envision applying methods for true site-specific glycoproteomics where the intact glycopeptide is analyzed by tandem mass spectrometry. This has already been investigated and applied for CSF by a few research groups, presenting data for the major CSF glycoproteins [111, 113, 119], and relevant aspects of glycoproteomics have also been reviewed [120-122]. However the methods for intact glycopeptide analysis are still not optimized for large scale analysis.

CONCLUSION

This study presents an in-depth analysis of the CSF proteome, comparing RRMS patients and neurological controls, and reports the largest set of quantified proteins and deglycopeptides in CSF to date. Pathway analyses of significantly changed proteins between the compared groups highlight biological processes that can be linked to MS pathology like inflammation, ECM organization, cell adhesion, immune system processes and neuron development. Of the clusters of changed proteins, cadherins, collagens, complement and proteoglycans were among those that appeared from the analysis, and these can also to a large degree be linked to the biological processes found changed. The correlating information from the pathway and cluster analysis gives a deep insight into the CNS processes affected by RRMS reflected in the CSF proteome. Many disease specific changes found among the deglycopeptides where the global protein abundance was not affected indicate that glycosylation status is affected by MS, and this group of proteins reveals a new level of information in the CNS pathology. Our study confirms many of the previously observed proteins changed by RRMS, but also reveals many new biomarker candidates that will be interesting to include in future verification studies.

ACKNOWLEDGEMENTS

The project is supported by the Kristian Gerhard Jebsen Foundation. H.B. is supported by the Bergen Research Foundation and the Research Council of Norway.

ABBREVIATIONS

AD	Alzheimer's disease
AGC	automatic gain control
APP	amyloid-beta A4 protein
BBB	blood-brain-barrier
CDMS	clinically definite multiple sclerosis
CHI3L1	chitinase-3-like protein 1
CHI3L2	chitinase-3-like protein 2
CIS	clinically isolated syndrome
CNS	central nervous system
CSF	cerebrospinal fluid
DTT	dithiothreitol
ECM	extracellular matrix
EDSS	expanded disability status scale
EGFR	epidermal growth factor receptor
FA	formic acid
FC	fold change
FDR	false discovery rate
GO	gene ontology
HCD	higher energy collision dissociation
IAA	iodoacetamide
Ig	immunoglobulin
IT	injection time
LP	lumbar puncture
MRI	magnetic resonance imaging
MS	multiple sclerosis
NFL	neurofilament light polypeptide
NOG	N-Octyl-β-D-glucopyranoside
OCB	oligoclonal band
OMgp	oligo-myelin glycoprotein
OND	other neurological disease
PD	Parkinson's disease
PG	proteoglycan
PNGase F	peptide -N-Glycosidase F
PPI	protein-protein interaction
RRMS	relapsing-remitting multiple sclerosis
TMT	tandem mass tag

SUPPORTING INFORMATION

Supplemental Information. Categorization of significant deglycopeptides, literature data inclusion criteria and categorization of literature studies.

Table S1. Detailed information for the patients and controls included in the CSF pools. RRMS patients are in sheet A and controls in sheet B. This table also indicates which of the included samples that have been used by our group in previous studies.

Table S2. LC-gradient and peptide fraction collection information.

Table S3. LC-gradient for LC-MS/MS analysis for the global data and the glycoproteome data.

Table S4. Data from the global proteome analysis. Default protein export from Reporter (sheet A), and all quantified proteins (sheet B).

Table S5. Data from the glycoproteome analysis. Default peptide export (sheet A), all quantified peptides (sheet B), all deglycopeptides (sheet C), all high confident deglycopeptides (sheet D), all deglycopeptides with significant p-value (sheet E), all deglycopeptides with significant p-value and z-score (sheet F), all category 1 significant deglycopeptides (sheet G) and all deglycopeptides also found as non-glycosylated in the global dataset (sheet H).

Table S6: 484 significant proteins from the global proteome analysis (sheet A). Sheet A also indicates which of the significant proteins that previously have been found in serum/plasma. The proteins included in the STRING network and in the ClueGO analysis is shown in sheet B.

Table S7. 49 category 1 deglycopeptides with significant p-value and z-score.

Table S8. Comparison of fold change deglycopeptides vs. global protein. . Details for significant peptide/protein comparison (sheet A), comparison plot significant peptide/protein comparison (sheet B), details for all peptide/protein comparison (sheet A), comparison plot all peptide/protein comparison (sheet B).

Table S9. Enriched biological processes in ClueGO. Global data.

Table S10. Enriched biological processes in ClueGO. Glycoproteome data.

Figure S1. Clusters generated in ClusterONE with p-value < 0.05.

PRIDE

Reviewer account details for the glycoproteome data:

Username: reviewer33108@ebi.ac.uk

Password: 9QdnugTQ

Reviewer account details for the global proteome data:

Username: reviewer13463@ebi.ac.uk

Password: DD0Y8UMs

REFERENCES

1. Compston, A.; Coles, A. Multiple sclerosis. *Lancet.* **2008**, *372*, 1502-1517.
2. Handel, A. E.; Giovannoni, G.; Ebers, G. C.; Ramagopalan, S. V. Environmental factors and their timing in adult-onset multiple sclerosis. *Nat Rev Neurol.* **2010**, *6*, 156-166.
3. Hedstrom, A. K.; Sundqvist, E.; Baarnhielm, M.; Nordin, N.; Hillert, J.; Kockum, I.; Olsson, T.; Alfredsson, L. Smoking and two human leukocyte antigen genes interact to increase the risk for multiple sclerosis. *Brain.* **2011**, *134*, 653-664.
4. Harris, V. K.; Sadiq, S. A. Biomarkers of therapeutic response in multiple sclerosis: current status. *Mol Diagn Ther.* **2014**, *18*, 605-617.
5. Piehl, F. A changing treatment landscape for multiple sclerosis: challenges and opportunities. *J Intern Med.* **2014**, *275*, 364-381.
6. Kappos, L.; Freedman, M. S.; Polman, C. H.; Edan, G.; Hartung, H. P.; Miller, D. H.; Montalban, X.; Barkhof, F.; Radu, E. W.; Metzig, C.; Bauer, L.; Lanius, V.; Sandbrink, R.; Pohl, C.; Group, B. S. Long-term effect of early treatment with interferon beta-1b after a first clinical event suggestive of multiple sclerosis: 5-year active treatment extension of the phase 3 BENEFIT trial. *Lancet Neurol.* **2009**, *8*, 987-997.
7. Rudick, R. A.; Polman, C. H. Current approaches to the identification and management of breakthrough disease in patients with multiple sclerosis. *Lancet Neurol.* **2009**, *8*, 545-559.
8. Polman, C. H.; O'Connor, P. W.; Havrdova, E.; Hutchinson, M.; Kappos, L.; Miller, D. H.; Phillips, J. T.; Lublin, F. D.; Giovannoni, G.; Wajgt, A.; Toal, M.; Lynn, F.; Panzara, M. A.; Sandrock, A. W.; Investigators, A. A randomized, placebo-controlled trial of natalizumab for relapsing multiple sclerosis. *N Engl J Med.* **2006**, *354*, 899-910.
9. Rudick, R. A.; Stuart, W. H.; Calabresi, P. A.; Confavreux, C.; Galetta, S. L.; Radue, E. W.; Lublin, F. D.; Weinstock-Guttman, B.; Wynn, D. R.; Lynn, F.; Panzara, M. A.; Sandrock, A. W.; Investigators, S. Natalizumab plus interferon beta-1a for relapsing multiple sclerosis. *N Engl J Med.* **2006**, *354*, 911-923.
10. Atkins, H. L.; Bowman, M.; Allan, D.; Anstee, G.; Arnold, D. L.; Bar-Or, A.; Bence-Bruckler, I.; Birch, P.; Bredeson, C.; Chen, J.; Fergusson, D.; Halpenny, M.; Hamelin, L.; Huebsch, L.; Hutton, B.; Laneuville, P.; Lapierre, Y.; Lee, H.; Martin, L.; McDiarmid, S.; O'Connor, P.; Ramsay, T.; Sabloff, M.; Walker, L.; Freedman, M. S. Immunoablation and autologous haemopoietic stem-cell transplantation for aggressive multiple sclerosis: a multicentre single-group phase 2 trial. *Lancet.* **2016**, *388*, 576-585.
11. Bakhuraysah, M. M.; Siatskas, C.; Petratos, S. Hematopoietic stem cell transplantation for multiple sclerosis: is it a clinical reality? *Stem Cell Res Ther.* **2016**, *7*, 12.
12. Brown, P.; Davies, S.; Speake, T.; Millar, I. Molecular mechanisms of cerebrospinal fluid production. *Neuroscience.* **2004**, *129*, 957-970.
13. Comabella, M.; Fernandez, M.; Martin, R.; Rivera-Vallve, S.; Borras, E.; Chiva, C.; Julia, E.; Rovira, A.; Canto, E.; Alvarez-Cermeno, J. C.; Villar, L. M.; Tintore, M.;

Montalban, X. Cerebrospinal fluid chitinase 3-like 1 levels are associated with conversion to multiple sclerosis. *Brain.* **2010**, *133*, 1082-1093.

14. Stoop, M. P.; Singh, V.; Stingl, C.; Martin, R.; Khademi, M.; Olsson, T.; Hintzen, R. Q.; Luider, T. M. Effects of natalizumab treatment on the cerebrospinal fluid proteome of multiple sclerosis patients. *J Proteome Res.* **2013**, *12*, 1101-1107.

15. Kroksveen, A. C.; Opsahl, J. A.; Guldbrandsen, A.; Myhr, K. M.; Oveland, E.; Torkildsen, O.; Berven, F. S. Cerebrospinal fluid proteomics in multiple sclerosis. *Biochim Biophys Acta.* **2015**, *1854*, 746-756.

16. Guldbrandsen, A.; Vethe, H.; Farag, Y.; Oveland, E.; Garberg, H.; Berle, M.; Myhr, K. M.; Opsahl, J. A.; Barsnes, H.; Berven, F. S. In-depth characterization of the cerebrospinal fluid (CSF) proteome displayed through the CSF proteome resource (CSF-PR). *Mol Cell Proteomics.* **2014**, *13*, 3152-3163.

17. Zhang, Y.; Guo, Z.; Zou, L.; Yang, Y.; Zhang, L.; Ji, N.; Shao, C.; Sun, W.; Wang, Y. A comprehensive map and functional annotation of the normal human cerebrospinal fluid proteome. *J Proteomics.* **2015**, *119*, 90-99.

18. Shepard, H. M.; Lewis, G. D.; Sarup, J. C.; Fendly, B. M.; Maneval, D.; Mordenti, J.; Figari, I.; Kotts, C. E.; Palladino, M. A., Jr.; Ullrich, A.; et al. Monoclonal antibody therapy of human cancer: taking the HER2 protooncogene to the clinic. *J Clin Immunol.* **1991**, *11*, 117-127.

19. Opdenakker, G.; Dillen, C.; Fiten, P.; Martens, E.; Van Aelst, I.; Van den Steen, P. E.; Nelissen, I.; Starckx, S.; Descamps, F. J.; Hu, J.; Piccard, H.; Van Damme, J.; Wormald, M. R.; Rudd, P. M.; Dwek, R. A. Remnant epitopes, autoimmunity and glycosylation. *Biochim Biophys Acta.* **2006**, *1760*, 610-615.

20. Mkhikian, H.; Grigorian, A.; Li, C. F.; Chen, H. L.; Newton, B.; Zhou, R. W.; Beeton, C.; Torossian, S.; Tatarian, G. G.; Lee, S. U.; Lau, K.; Walker, E.; Siminovitch, K. A.; Chandy, K. G.; Yu, Z.; Dennis, J. W.; Demetriou, M. Genetics and the environment converge to dysregulate N-glycosylation in multiple sclerosis. *Nat Commun.* **2011**, *2*, 334.

21. Grigorian, A.; Mkhikian, H.; Li, C. F.; Newton, B. L.; Zhou, R. W.; Demetriou, M. Pathogenesis of multiple sclerosis via environmental and genetic dysregulation of N-glycosylation. *Semin Immunopathol.* **2012**, *34*, 415-424.

22. Teunissen, C. E.; Petzold, A.; Bennett, J. L.; Berven, F. S.; Brundin, L.; Comabella, M.; Franciotta, D.; Frederiksen, J. L.; Fleming, J. O.; Furlan, R.; Hintzen, R. Q.; Hughes, S. G.; Johnson, M. H.; Krasulova, E.; Kuhle, J.; Magnone, M. C.; Rajda, C.; Rejdak, K.; Schmidt, H. K.; van Pesch, V.; Waubant, E.; Wolf, C.; Giovannoni, G.; Hemmer, B.; Tumani, H.; Deisenhammer, F. A consensus protocol for the standardization of cerebrospinal fluid collection and biobanking. *Neurology.* **2009**, *73*, 1914-1922.

23. Polman, C. H.; Reingold, S. C.; Edan, G.; Filippi, M.; Hartung, H. P.; Kappos, L.; Lublin, F. D.; Metz, L. M.; McFarland, H. F.; O'Connor, P. W.; Sandberg-Wollheim, M.; Thompson, A. J.; Weinshenker, B. G.; Wolinsky, J. S. Diagnostic criteria for multiple sclerosis: 2005 Revisions to the "McDonald Criteria". *Annals of Neurology.* **2005**, *58*, 840-846.

24. Aasebo, E.; Opsahl, J. A.; Bjorlykke, Y.; Myhr, K. M.; Kroksveen, A. C.; Berven, F. S. Effects of blood contamination and the rostro-caudal gradient on the human cerebrospinal fluid proteome. *PLoS One.* **2014**, *9*, e90429.

25. Kroksveen, A. C.; Aasebo, E.; Vethe, H.; Van Pesch, V.; Franciotta, D.; Teunissen, C. E.; Ulvik, R. J.; Vedeler, C.; Myhr, K. M.; Barsnes, H.; Berven, F. S. Discovery and initial verification of differentially abundant proteins between multiple sclerosis patients and controls using iTRAQ and SID-SRM. *J Proteomics.* **2013**, *78*, 312-325.

26. Guldbrandsen, A.; Barsnes, H.; Kroksveen, A. C.; Berven, F. S.; Vaudel, M. A Simple Workflow for Large Scale Shotgun Glycoproteomics. *Methods Mol Biol.* **2016**, *1394*, 275-286.

27. Olsen, J. V.; de Godoy, L. M.; Li, G.; Macek, B.; Mortensen, P.; Pesch, R.; Makarov, A.; Lange, O.; Horning, S.; Mann, M. Parts per million mass accuracy on an Orbitrap mass spectrometer via lock mass injection into a C-trap. *Mol. Cell. Proteomics.* **2005**, *4*, 2010-2021.

28. Kessner, D.; Chambers, M.; Burke, R.; Agus, D.; Mallick, P. ProteoWizard: open source software for rapid proteomics tools development. *Bioinformatics.* **2008**, *24*, 2534-2536.

29. Craig, R.; Beavis, R. C. TANDEM: matching proteins with tandem mass spectra. *Bioinformatics.* **2004**, *20*, 1466-1467.

30. Tabb, D. L.; Fernando, C. G.; Chambers, M. C. MyriMatch: highly accurate tandem mass spectral peptide identification by multivariate hypergeometric analysis. *J Proteome Res.* **2007**, *6*, 654-661.

31. Eng, J. K.; Jahan, T. A.; Hoopmann, M. R. Comet: an open-source MS/MS sequence database search tool. *Proteomics.* **2013**, *13*, 22-24.

32. Vaudel, M.; Barsnes, H.; Berven, F. S.; Sickmann, A.; Martens, L. SearchGUI: An open-source graphical user interface for simultaneous OMSSA and X!Tandem searches. *Proteomics.* **2011**, *11*, 996-999.

33. Apweiler, R.; Bairoch, A.; Wu, C. H.; Barker, W. C.; Boeckmann, B.; Ferro, S.; Gasteiger, E.; Huang, H.; Lopez, R.; Magrane, M.; Martin, M. J.; Natale, D. A.; O'Donovan, C.; Redaschi, N.; Yeh, L. S. UniProt: the Universal Protein knowledgebase. *Nucleic Acids Res.* **2004**, *32*, D115-119.

34. Vaudel, M.; Burkhart, J. M.; Zahedi, R. P.; Oveland, E.; Berven, F. S.; Sickmann, A.; Martens, L.; Barsnes, H. PeptideShaker enables reanalysis of MS-derived proteomics data sets. *Nat Biotechnol.* **2015**, *33*, 22-24.

35. Nesvizhskii, A. I.; Aebersold, R. Interpretation of shotgun proteomic data: the protein inference problem. *Mol Cell Proteomics.* **2005**, *4*, 1419-1440.

36. Elias, J. E.; Gygi, S. P. Target-decoy search strategy for mass spectrometry-based proteomics. *Methods Mol. Biol.* **2010**, *604*, 55-71.

37. Vaudel, M.; Breiter, D.; Beck, F.; Rahnenfuhrer, J.; Martens, L.; Zahedi, R. P. D-score: a search engine independent MD-score. *Proteomics.* **2013**, *13*, 1036-1041.

38. Taus, T.; Kocher, T.; Pichler, P.; Paschke, C.; Schmidt, A.; Henrich, C.; Mechtler, K. Universal and confident phosphorylation site localization using phosphoRS. *J. Proteome Res.* **2011**, *10*, 5354-5362.

39. Burkhart, J. M.; Vaudel, M.; Zahedi, R. P.; Martens, L.; Sickmann, A. iTRAQ protein quantification: a quality-controlled workflow. *Proteomics.* **2011**, *11*, 1125-1134.

40. Vaudel, M.; Sickmann, A.; Martens, L. Introduction to opportunities and pitfalls in functional mass spectrometry based proteomics. *Biochim Biophys Acta.* **2014**, *1844*, 12-20.

41. Opsahl, J. A.; Vaudel, M.; Guldbrandsen, A.; Aasebo, E.; Van Pesch, V.; Franciotta, D.; Myhr, K. M.; Barsnes, H.; Berle, M.; Torkildsen, O.; Kroksveen, A. C.; Berven, F. S. Label-free analysis of human cerebrospinal fluid addressing various normalization strategies and revealing protein groups affected by multiple sclerosis. *Proteomics.* **2016**, *16*, 1154-1165.

42. Tian, Y.; Zhou, Y.; Elliott, S.; Aebersold, R.; Zhang, H. Solid-phase extraction of N-linked glycopeptides. *Nat Protoc.* **2007**, *2*, 334-339.

43. Vizcaino, J. A.; Deutsch, E. W.; Wang, R.; Csordas, A.; Reisinger, F.; Rios, D.; Dianes, J. A.; Sun, Z.; Farrah, T.; Bandeira, N.; Binz, P. A.; Xenarios, I.; Eisenacher, M.; Mayer, G.; Gatto, L.; Campos, A.; Chalkley, R. J.; Kraus, H. J.; Albar, J. P.; Martinez-Bartolome, S.; Apweiler, R.; Omenn, G. S.; Martens, L.; Jones, A. R.; Hermjakob, H. ProteomeXchange provides globally coordinated proteomics data submission and dissemination. *Nat Biotechnol.* **2014**, *32*, 223-226.

44. Vizcaino, J. A.; Csordas, A.; del-Toro, N.; Dianes, J. A.; Griss, J.; Lavidas, I.; Mayer, G.; Perez-Riverol, Y.; Reisinger, F.; Ternent, T.; Xu, Q. W.; Wang, R.; Hermjakob, H. 2016 update of the PRIDE database and its related tools. *Nucleic Acids Res.* **2016**, *44*, D447-456.

45. Szklarczyk, D.; Franceschini, A.; Wyder, S.; Forslund, K.; Heller, D.; Huerta-Cepas, J.; Simonovic, M.; Roth, A.; Santos, A.; Tsafou, K. P.; Kuhn, M.; Bork, P.; Jensen, L. J.; von Mering, C. STRING v10: protein-protein interaction networks, integrated over the tree of life. *Nucleic Acids Res.* **2015**, *43*, D447-452.

46. Shannon, P.; Markiel, A.; Ozier, O.; Baliga, N. S.; Wang, J. T.; Ramage, D.; Amin, N.; Schwikowski, B.; Ideker, T. Cytoscape: a software environment for integrated models of biomolecular interaction networks. *Genome Res.* **2003**, *13*, 2498-2504.

47. Maere, S.; Heymans, K.; Kuiper, M. BiNGO: a Cytoscape plugin to assess overrepresentation of gene ontology categories in biological networks. *Bioinformatics.* **2005**, *21*, 3448-3449.

48. Nepusz, T.; Yu, H.; Paccanaro, A. Detecting overlapping protein complexes in protein-protein interaction networks. *Nat Methods.* **2012**, *9*, 471-472.

49. Bindea, G.; Mlecnik, B.; Hackl, H.; Charoentong, P.; Tosolini, M.; Kirilovsky, A.; Fridman, W. H.; Pages, F.; Trajanoski, Z.; Galon, J. ClueGO: a Cytoscape plug-in to decipher functionally grouped gene ontology and pathway annotation networks. *Bioinformatics.* **2009**, *25*, 1091-1093.

50. Bindea, G.; Galon, J.; Mlecnik, B. CluePedia Cytoscape plugin: pathway insights using integrated experimental and in silico data. *Bioinformatics.* **2013**, *29*, 661-663.

51. Borras, E.; Canto, E.; Choi, M.; Maria Villar, L.; Alvarez-Cermeno, J. C.; Chiva, C.; Montalban, X.; Vitek, O.; Comabella, M.; Sabido, E. Protein-Based Classifier to Predict Conversion from Clinically Isolated Syndrome to Multiple Sclerosis. *Mol Cell Proteomics.* **2016**, *15*, 318-328.

52. Kroksveen, A. C.; Jaffe, J. D.; Aasebo, E.; Barsnes, H.; Bjorlykke, Y.; Franciotta, D.; Keshishian, H.; Myhr, K. M.; Opsahl, J. A.; van Pesch, V.; Teunissen, C. E.; Torkildsen, O.; Ulvik, R. J.; Vethe, H.; Carr, S. A.; Berven, F. S. Quantitative

proteomics suggests decrease in the secretogranin-1 cerebrospinal fluid levels during the disease course of multiple sclerosis. *Proteomics.* **2015**, *15*, 3361-3369.

53. Hinsinger, G.; Galeotti, N.; Nabholz, N.; Urbach, S.; Rigau, V.; Demattei, C.; Lehmann, S.; Camu, W.; Labauge, P.; Castelnovo, G.; Brassat, D.; Loussouarn, D.; Salou, M.; Laplaud, D.; Casez, O.; Bockaert, J.; Marin, P.; Thouvenot, E. Chitinase 3-like proteins as diagnostic and prognostic biomarkers of multiple sclerosis. *Mult Scler.* **2015**, *21*, 1251-1261.

54. Canto, E.; Tintore, M.; Villar, L. M.; Borras, E.; Alvarez-Cermeno, J. C.; Chiva, C.; Sabido, E.; Rovira, A.; Montalban, X.; Comabella, M. Validation of semaphorin 7A and ala-beta-his-dipeptidase as biomarkers associated with the conversion from clinically isolated syndrome to multiple sclerosis. *J Neuroinflammation.* **2014**, *11*, 181.

55. Schutzer, S. E.; Angel, T. E.; Liu, T.; Schepmoes, A. A.; Xie, F.; Bergquist, J.; Vecsei, L.; Zadori, D.; Camp, D. G., 2nd; Holland, B. K.; Smith, R. D.; Coyle, P. K. Gray matter is targeted in first-attack multiple sclerosis. *PLoS One.* **2013**, *8*, e66117.

56. Kroksveen, A. C.; Guldbrandsen, A.; Vedeler, C.; Myhr, K. M.; Opsahl, J. A.; Berven, F. S. Cerebrospinal fluid proteome comparison between multiple sclerosis patients and controls. *Acta Neurol Scand Suppl.* **2012**, 90-96.

57. Jia, Y.; Wu, T.; Jelinek, C. A.; Bielekova, B.; Chang, L.; Newsome, S.; Gnanapavan, S.; Giovannoni, G.; Chen, D.; Calabresi, P. A.; Nath, A.; Cotter, R. J. Development of protein biomarkers in cerebrospinal fluid for secondary progressive multiple sclerosis using selected reaction monitoring mass spectrometry (SRM-MS). *Clin Proteomics.* **2012**, *9*, 9.

58. Spellman, D. S.; Wildsmith, K. R.; Honigberg, L. A.; Tuefferd, M.; Baker, D.; Raghavan, N.; Nairn, A. C.; Croteau, P.; Schirm, M.; Allard, R.; Lamontagne, J.; Chelsky, D.; Hoffmann, S.; Potter, W. Z.; Alzheimer's Disease Neuroimaging, I.; Foundation for, N. I. H. B. C. C. S. F. P. P. T. Development and evaluation of a multiplexed mass spectrometry based assay for measuring candidate peptide biomarkers in Alzheimer's Disease Neuroimaging Initiative (ADNI) CSF. *Proteomics Clin Appl.* **2015**, *9*, 715-731.

59. Wildsmith, K. R.; Schauer, S. P.; Smith, A. M.; Arnott, D.; Zhu, Y.; Haznedar, J.; Kaur, S.; Mathews, W. R.; Honigberg, L. A. Identification of longitudinally dynamic biomarkers in Alzheimer's disease cerebrospinal fluid by targeted proteomics. *Mol Neurodegener.* **2014**, *9*, 22.

60. Barucker, C.; Sommer, A.; Beckmann, G.; Eravci, M.; Harmeier, A.; Schipke, C. G.; Brockschnieder, D.; Dyrks, T.; Althoff, V.; Fraser, P. E.; Hazrati, L. N.; George-Hyslop, P. S.; Breitner, J. C.; Peters, O.; Multhaup, G. Alzheimer amyloid peptide abeta42 regulates gene expression of transcription and growth factors. *J Alzheimers Dis.* **2015**, *44*, 613-624.

61. Heywood, W. E.; Galimberti, D.; Bliss, E.; Sirka, E.; Paterson, R. W.; Magdalinou, N. K.; Carecchio, M.; Reid, E.; Heslegrave, A.; Fenoglio, C.; Scarpini, E.; Schott, J. M.; Fox, N. C.; Hardy, J.; Bhatia, K.; Heales, S.; Sebire, N. J.; Zetterberg, H.; Mills, K. Identification of novel CSF biomarkers for neurodegeneration and their validation by a high-throughput multiplexed targeted proteomic assay. *Mol Neurodegener.* **2015**, *10*, 64.

62. Shi, M.; Movius, J.; Dator, R.; Aro, P.; Zhao, Y.; Pan, C.; Lin, X.; Bammler, T. K.; Stewart, T.; Zabetian, C. P.; Peskind, E. R.; Hu, S. C.; Quinn, J. F.; Galasko, D. R.;

Zhang, J. Cerebrospinal fluid peptides as potential Parkinson disease biomarkers: a staged pipeline for discovery and validation. *Mol Cell Proteomics.* **2015**, *14*, 544-555.

63. Lehnert, S.; Jesse, S.; Rist, W.; Steinacker, P.; Soininen, H.; Herukka, S. K.; Tumani, H.; Lenter, M.; Oeckl, P.; Ferger, B.; Hengerer, B.; Otto, M. iTRAQ and multiple reaction monitoring as proteomic tools for biomarker search in cerebrospinal fluid of patients with Parkinson's disease dementia. *Exp Neurol.* **2012**, *234*, 499-505.

64. Kamimura, D. A., Y.; Atsumi, T.; Meng, J.; Sabharwal, L.; Bando, H.; Ogura, H.; Jiang, J. J.; Huseby, E. S.; Murakami, M. Role of cytokine-mediated crosstalk between T cells and noniimune cells in the pathophysiology og multiple sclerosis. In *Multiple sclerosis: a mechanistic view*, 1 ed.; Minagar, A., Ed. Academic Press: 2015; pp 101-125.

65. Erschbamer, M.; Pernold, K.; Olson, L. Inhibiting epidermal growth factor receptor improves structural, locomotor, sensory, and bladder recovery from experimental spinal cord injury. *J. Neurosci.* **2007**, *27*, 6428-6435.

66. Liu, B.; Chen, H.; Johns, T. G.; Neufeld, A. H. Epidermal growth factor receptor activation: an upstream signal for transition of quiescent astrocytes into reactive astrocytes after neural injury. *J Neurosci.* **2006**, *26*, 7532-7540.

67. O'Brien, R. J.; Wong, P. C. Amyloid precursor protein processing and Alzheimer's disease. *Annu Rev Neurosci.* **2011**, *34*, 185-204.

68. Lue, L. F.; Kuo, Y. M.; Roher, A. E.; Brachova, L.; Shen, Y.; Sue, L.; Beach, T.; Kurth, J. H.; Rydel, R. E.; Rogers, J. Soluble amyloid beta peptide concentration as a predictor of synaptic change in Alzheimer's disease. *Am J Pathol.* **1999**, *155*, 853-862.

69. Karp, N. A.; Lilley, K. S. Investigating sample pooling strategies for DIGE experiments to address biological variability. *Proteomics.* **2009**, *9*, 388-397.

70. Diz, A. P.; Truebano, M.; Skibinski, D. O. The consequences of sample pooling in proteomics: an empirical study. *Electrophoresis.* **2009**, *30*, 2967-2975.

71. Canto, E.; Tintore, M.; Villar, L. M.; Costa, C.; Nurtdinov, R.; Alvarez-Cermeno, J. C.; Arrambide, G.; Reverter, F.; Deisenhammer, F.; Hegen, H.; Khademi, M.; Olsson, T.; Tumani, H.; Rodriguez-Martin, E.; Piehl, F.; Bartos, A.; Zimova, D.; Kotoucova, J.; Kuhle, J.; Kappos, L.; Garcia-Merino, J. A.; Sanchez, A. J.; Saiz, A.; Blanco, Y.; Hintzen, R.; Jafari, N.; Brassat, D.; Lauda, F.; Roesler, R.; Rejdak, K.; Papuc, E.; de Andres, C.; Rauch, S.; Khalil, M.; Enzinger, C.; Galimberti, D.; Scarpini, E.; Teunissen, C.; Sanchez, A.; Rovira, A.; Montalban, X.; Comabella, M. Chitinase 3-like 1: prognostic biomarker in clinically isolated syndromes. *Brain.* **2015**, *138*, 918-931.

72. Modvig, S.; Degn, M.; Roed, H.; Sorensen, T. L.; Larsson, H. B.; Langkilde, A. R.; Frederiksen, J. L.; Sellebjerg, F. Cerebrospinal fluid levels of chitinase 3-like 1 and neurofilament light chain predict multiple sclerosis development and disability after optic neuritis. *Mult Scler.* **2015**, *21*, 1761-1770.

73. Kuhle, J.; Malmestrom, C.; Axelsson, M.; Plattner, K.; Yaldizli, O.; Derfuss, T.; Giovannoni, G.; Kappos, L.; Lycke, J. Neurofilament light and heavy subunits compared as therapeutic biomarkers in multiple sclerosis. *Acta Neurol Scand.* **2013**, *128*, e33-36.

74. Canto, E.; Reverter, F.; Morcillo-Suarez, C.; Matesanz, F.; Fernandez, O.; Izquierdo, G.; Vandenbroeck, K.; Rodriguez-Antiguedad, A.; Urcelay, E.; Arroyo, R.; Otaegui,

D.; Olascoaga, J.; Saiz, A.; Navarro, A.; Sanchez, A.; Dominguez, C.; Caminero, A.; Horga, A.; Tintore, M.; Montalban, X.; Comabella, M. Chitinase 3-like 1 plasma levels are increased in patients with progressive forms of multiple sclerosis. *Mult Scler.* **2012**, *18*, 983-990.

75. Disanto, G.; Adiutori, R.; Dobson, R.; Martinelli, V.; Dalla Costa, G.; Runia, T.; Evdoshenko, E.; Thouvenot, E.; Trojano, M.; Norgren, N.; Teunissen, C.; Kappos, L.; Giovannoni, G.; Kuhle, J.; International Clinically Isolated Syndrome Study, G. Serum neurofilament light chain levels are increased in patients with a clinically isolated syndrome. *J Neurol Neurosurg Psychiatry.* **2016**, *87*, 126-129.

76. Muthusamy, B.; Hanumanthu, G.; Suresh, S.; Rekha, B.; Srinivas, D.; Karthick, L.; Vrushabendra, B. M.; Sharma, S.; Mishra, G.; Chatterjee, P.; Mangala, K. S.; Shivashankar, H. N.; Chandrika, K. N.; Deshpande, N.; Suresh, M.; Kannabiran, N.; Niranjan, V.; Nalli, A.; Prasad, T. S.; Arun, K. S.; Reddy, R.; Chandran, S.; Jadhav, T.; Julie, D.; Mahesh, M.; John, S. L.; Palvankar, K.; Sudhir, D.; Bala, P.; Rashmi, N. S.; Vishnupriya, G.; Dhar, K.; Reshma, S.; Chaerkady, R.; Gandhi, T. K.; Harsha, H. C.; Mohan, S. S.; Deshpande, K. S.; Sarker, M.; Pandey, A. Plasma Proteome Database as a resource for proteomics research. *Proteomics.* **2005**, *5*, 3531-3536.

77. Lucchinetti, C.; Bruck, W.; Parisi, J.; Scheithauer, B.; Rodriguez, M.; Lassmann, H. Heterogeneity of multiple sclerosis lesions: implications for the pathogenesis of demyelination. *Ann Neurol.* **2000**, *47*, 707-717.

78. Hemmer, B.; Kerschensteiner, M.; Korn, T. Role of the innate and adaptive immune responses in the course of multiple sclerosis. *Lancet Neurol.* **2015**, *14*, 406-419.

79. Engelhardt, B.; Ransohoff, R. M. Capture, crawl, cross: the T cell code to breach the blood-brain barriers. *Trends Immunol.* **2012**, *33*, 579-589.

80. Kindt, T. J.; Goldsby, R. A.; Osborne, B. A. Innate Immunity. In *Immunology*, Sixth ed.; W.H. Freeman and Company: New York, 2007; pp 57-59.

81. Breij, E. C.; Brink, B. P.; Veerhuis, R.; van den Berg, C.; Vloet, R.; Yan, R.; Dijkstra, C. D.; van der Valk, P.; Bo, L. Homogeneity of active demyelinating lesions in established multiple sclerosis. *Ann Neurol.* **2008**, *63*, 16-25.

82. Avsar, T.; Durasi, I. M.; Uygunoglu, U.; Tutuncu, M.; Demirci, N. O.; Saip, S.; Sezerman, O. U.; Siva, A.; Tahir Turanli, E. CSF Proteomics Identifies Specific and Shared Pathways for Multiple Sclerosis Clinical Subtypes. *PLoS One.* **2015**, *10*, e0122045.

83. Han, M. H.; Hwang, S. I.; Roy, D. B.; Lundgren, D. H.; Price, J. V.; Ousman, S. S.; Fernald, G. H.; Gerlitz, B.; Robinson, W. H.; Baranzini, S. E.; Grinnell, B. W.; Raine, C. S.; Sobel, R. A.; Han, D. K.; Steinman, L. Proteomic analysis of active multiple sclerosis lesions reveals therapeutic targets. *Nature.* **2008**, *451*, 1076-1081.

84. Sheremata, W. A.; Jy, W.; Horstman, L. L.; Ahn, Y. S.; Alexander, J. S.; Minagar, A. Evidence of platelet activation in multiple sclerosis. *J Neuroinflammation.* **2008**, *5*, 27.

85. Ruggeri, Z. M.; Mendolicchio, G. L. Adhesion mechanisms in platelet function. *Circ Res.* **2007**, *100*, 1673-1685.

86. Semple, J. W.; Italiano, J. E., Jr.; Freedman, J. Platelets and the immune continuum. *Nat Rev Immunol.* **2011**, *11*, 264-274.

87. Terranova, V. P.; Rohrbach, D. H.; Martin, G. R. Role of laminin in the attachment of PAM 212 (epithelial) cells to basement membrane collagen. *Cell.* **1980**, *22*, 719-726.

88. Spiegel, M.; Kruger, H.; Hofmann, E.; Kappos, L. MRI study of Balo's concentric sclerosis before and after immunosuppressive therapy. *J Neurol.* **1989**, *236*, 487-488.

89. Mohan, H.; Krumbholz, M.; Sharma, R.; Eisele, S.; Junker, A.; Sixt, M.; Newcombe, J.; Wekerle, H.; Hohlfeld, R.; Lassmann, H.; Meinl, E. Extracellular matrix in multiple sclerosis lesions: Fibrillar collagens, biglycan and decorin are upregulated and associated with infiltrating immune cells. *Brain Pathol.* **2010**, *20*, 966-975.

90. Rhodes, K. E.; Fawcett, J. W. Chondroitin sulphate proteoglycans: preventing plasticity or protecting the CNS? *J. Anat.* **2004**, *204*, 33-48.

91. Sobel, R. A. The extracellular matrix in multiple sclerosis lesions. *J Neuropathol Exp Neurol.* **1998**, *57*, 205-217.

92. van Horssen, J.; Dijkstra, C. D.; de Vries, H. E. The extracellular matrix in multiple sclerosis pathology. *J Neurochem.* **2007**, *103*, 1293-1301.

93. Coen, M.; Menegatti, E.; Salvi, F.; Mascoli, F.; Zamboni, P.; Gabbiani, G.; Bochaton-Piallat, M. L. Altered collagen expression in jugular veins in multiple sclerosis. *Cardiovasc Pathol.* **2013**, *22*, 33-38.

94. Cui, H.; Freeman, C.; Jacobson, G. A.; Small, D. H. Proteoglycans in the central nervous system: role in development, neural repair, and Alzheimer's disease. *IUBMB Life.* **2013**, *65*, 108-120.

95. Levine, J. M. Increased expression of the NG2 chondroitin-sulfate proteoglycan after brain injury. *J Neurosci.* **1994**, *14*, 4716-4730.

96. Properzi, F.; Fawcett, J. W. Proteoglycans and brain repair. *News Physiol Sci.* **2004**, *19*, 33-38.

97. Sobel, R. A.; Ahmed, A. S. White matter extracellular matrix chondroitin sulfate/dermatan sulfate proteoglycans in multiple sclerosis. *J Neuropathol Exp Neurol.* **2001**, *60*, 1198-1207.

98. Borges, I. T.; Shea, C. D.; Ohayon, J.; Jones, B. C.; Stone, R. D.; Ostuni, J.; Shiee, N.; McFarland, H.; Bielekova, B.; Reich, D. S. The effect of daclizumab on brain atrophy in relapsing-remitting multiple sclerosis. *Mult Scler Relat Disord.* **2013**, *2*, 133-140.

99. De Stefano, N.; Narayanan, S.; Francis, G. S.; Arnaoutelis, R.; Tartaglia, M. C.; Antel, J. P.; Matthews, P. M.; Arnold, D. L. Evidence of axonal damage in the early stages of multiple sclerosis and its relevance to disability. *Arch Neurol.* **2001**, *58*, 65-70.

100. Trapp, B. D.; Peterson, J.; Ransohoff, R. M.; Rudick, R.; Mork, S.; Bo, L. Axonal transection in the lesions of multiple sclerosis. *New England Journal of Medicine.* **1998**, *338*, 278-285.

101. Gunnarsson, M.; Malmeström, C.; Axelsson, M.; Sundström, P.; Dahle, C.; Vrethem, M.; Olsson, T.; Piehl, F.; Norgren, N.; Rosengren, L.; Svenningsson, A.; Lycke, J. Axonal damage in relapsing multiple sclerosis is markedly reduced by natalizumab. *Annals of neurology.* **2011**, *69*, 83-89.

102. Linneberg, C.; Harboe, M.; Laursen, L. S. Axo-Glia Interaction Preceding CNS Myelination Is Regulated by Bidirectional Eph-Ephrin Signaling. *ASN Neuro.* **2015**, *7*, 1-17.

103. Sobel, R. A. Ephrin A receptors and ligands in lesions and normal-appearing white matter in multiple sclerosis. *Brain Pathol.* **2005**, *15*, 35-45.

104. Stojanovic, I. R.; Kostic, M.; Ljubisavljevic, S. The role of glutamate and its receptors in multiple sclerosis. *J Neural Transm (Vienna).* **2014**, *121*, 945-955.

105. Takeichi, M. The cadherins: cell-cell adhesion molecules controlling animal morphogenesis. *Development.* **1988**, *102*, 639-655.

106. Klingener, M.; Chavali, M.; Singh, J.; McMillan, N.; Coomes, A.; Dempsey, P. J.; Chen, E. I.; Aguirre, A. N-cadherin promotes recruitment and migration of neural progenitor cells from the SVZ neural stem cell niche into demyelinated lesions. *J Neurosci.* **2014**, *34*, 9590-9606.

107. Hochmeister, S.; Romauch, M.; Bauer, J.; Seifert-Held, T.; Weissert, R.; Linington, C.; Hartung, H. P.; Fazekas, F.; Storch, M. K. Re-expression of N-cadherin in remyelinating lesions of experimental inflammatory demyelination. *Exp Neurol.* **2012**, *237*, 70-77.

108. Damotte, V.; Guillot-Noel, L.; Patsopoulos, N. A.; Madireddy, L.; El Behi, M.; International Multiple Sclerosis Genetics, C.; Wellcome Trust Case Control, C.; De Jager, P. L.; Baranzini, S. E.; Cournu-Rebeix, I.; Fontaine, B. A gene pathway analysis highlights the role of cellular adhesion molecules in multiple sclerosis susceptibility. *Genes Immun.* **2014**, *15*, 126-132.

109. Engelhardt, B. Immune cell entry into the central nervous system: involvement of adhesion molecules and chemokines. *J Neurol Sci.* **2008**, *274*, 23-26.

110. Pan, S.; Wang, Y.; Quinn, J. F.; Peskind, E. R.; Waichunas, D.; Wimberger, J. T.; Jin, J.; Li, J. G.; Zhu, D.; Pan, C.; Zhang, J. Identification of glycoproteins in human cerebrospinal fluid with a complementary proteomic approach. *J Proteome Res.* **2006**, *5*, 2769-2779.

111. Nilsson, J.; Ruetschi, U.; Halim, A.; Hesse, C.; Carlsohn, E.; Brinkmalm, G.; Larson, G. Enrichment of glycopeptides for glycan structure and attachment site identification. *Nat Methods.* **2009**, *6*, 809-811.

112. Halim, A.; Ruetschi, U.; Larson, G.; Nilsson, J. LC-MS/MS characterization of O-glycosylation sites and glycan structures of human cerebrospinal fluid glycoproteins. *J Proteome Res.* **2013**, *12*, 573-584.

113. Goyallon, A.; Cholet, S.; Chapelle, M.; Junot, C.; Fenaille, F. Evaluation of a combined glycomics and glycoproteomics approach for studying the major glycoproteins present in biofluids: Application to cerebrospinal fluid. *Rapid Commun Mass Spectrom.* **2015**, *29*, 461-473.

114. Filbin, M. T. Myelin-associated inhibitors of axonal regeneration in the adult mammalian CNS. *Nat Rev Neurosci.* **2003**, *4*, 703-713.

115. Wang, K. C.; Koprivica, V.; Kim, J. A.; Sivasankaran, R.; Guo, Y.; Neve, R. L.; He, Z. Oligodendrocyte-myelin glycoprotein is a Nogo receptor ligand that inhibits neurite outgrowth. *Nature.* **2002**, *417*, 941-944.

116. Kottis, V.; Thibault, P.; Mikol, D.; Xiao, Z. C.; Zhang, R.; Dergham, P.; Braun, P. E. Oligodendrocyte-myelin glycoprotein (OMgp) is an inhibitor of neurite outgrowth. *J Neurochem.* **2002**, *82*, 1566-1569.

117. Nakaya, N.; Sultana, A.; Lee, H. S.; Tomarev, S. I. Olfactomedin 1 interacts with the Nogo A receptor complex to regulate axon growth. *J Biol Chem.* **2012**, *287*, 37171-37184.

118. Schwab, M. E.; Strittmatter, S. M. Nogo limits neural plasticity and recovery from injury. *Curr Opin Neurobiol.* **2014**, *27*, 53-60.

119. Halim, A.; Westerlind, U.; Pett, C.; Schorlemer, M.; Ruetschi, U.; Brinkmalm, G.; Sihlbom, C.; Lengqvist, J.; Larson, G.; Nilsson, J. Assignment of saccharide identities through analysis of oxonium ion fragmentation profiles in LC-MS/MS of glycopeptides. *J Proteome Res.* **2014**, *13*, 6024-6032.

120. Nilsson, J.; Halim, A.; Grahn, A.; Larson, G. Targeting the glycoproteome. *Glycoconj J.* **2013**, *30*, 119-136.

121. Thaysen-Andersen, M.; Packer, N. H. Advances in LC-MS/MS-based glycoproteomics: getting closer to system-wide site-specific mapping of the N- and O-glycoproteome. *Biochim Biophys Acta.* **2014**, *1844*, 1437-1452.

122. Thaysen-Andersen, M.; Packer, N. H.; Schulz, B. L. Maturing Glycoproteomics Technologies Provide Unique Structural Insights into the N-glycoproteome and Its Regulation in Health and Disease. *Mol Cell Proteomics.* **2016**, *15*, 1773-1790.

LIST OF FIGURE LEGENDS

Figure 1. Illustration of the pooling procedure (A) and the workflow of global (B) and deglycoproteome (C) experiments performed in this study. The pooling procedure shown in Figure 1A illustrates that 21 relapsing-remitting multiple sclerosis (RRMS) patients and 21 neurological controls with other neurological diseases (OND) were separated into six pools, with seven individuals in each pool. These pools were used for two separate experiments: B) Global proteome analysis and C) Deglycoproteome analysis. Only the global experiment included protein depletion (B), while trypsin digestion, TMT labeling and combination of the labeled pools was common for both experiments. Glycopeptide capture by solid-phase enrichment of N-linked glycopeptides (SPEG) was then performed in the glycoproteome experiment (C), followed by peptide fractionation, LC-MS/MS analysis and protein and peptide identification and quantification, which was common for both experiments.

Figure 2: Distribution of protein data for proteins previously quantified in comparable CSF studies. Proteins found significantly increased (left) or decreased (right) in MS were compared separately to eight publications. Red circles represent the query proteins found increased in MS compared to Non-MS in 100% of the studies and pink circles represent the proteins found increased in MS in the majority of studies, but with some conflicting data. Green and light green circles represent these same trends for the decreased proteins. The blue circles represent the proteins found unaltered between MS and Non-MS on average in the seven studies. The MS category is a combination of the reported MS subcategories: RRMS, CDMS and CIS with conversion to MS, and the Non-MS category is a combination of the control group subcategories reported as OND, Symptomatic controls and Non-MS. More information about this categorization is in **Supplemental Information**. * Combined categories.

Figure 3. Biological processes GO enriched in proteins increased (A and B) and decreased (C and D) in CSF of RRMS patients. The global data is shown in A (increased in RRMS) and C (decreased in RRMS) and the glycoproteome data is shown in B (increased in RRMS) and D (decreased in RRMS).

Figure 4. Protein-protein interaction (PPI) network. 484 significantly changed proteins between the RRMS patients and the controls (Table S6) were imported into STRING [45] and interactions were found between 222 of the 484 proteins. The PPI was visualized in Cytoscape v3.3.0. Green and red colors represent lower and higher expression of proteins in CSF between RRMS patients and controls, respectively. Light green and light red represent proteins with z-score significance > 0.05, while the dark green and red proteins have z-score significance < 0.05. Rectangles are proteins with a t-test *p*-value < 0.01, while the proteins represented by a circle have *p*-value between 0.01 and 0.05.

Figure 5. Cluster analysis of the protein-protein interaction network using ClusterONE. A minimum of five genes was included in the network and interaction evidence towards the combined score from STRING. a) cadherins b) collagens c) complement proteins d) ephrins and proteins involved in synaptic plasticity e) proteins involved in aminoglycan processes f) proteins involved in the coagulation and inflammation. Green and red

colors represent lower and higher expression of proteins in CSF between RRMS patients and controls, respectively. Light green and light red represent proteins with z-score significance > 0.05, while the dark green and red proteins have z-score significance < 0.05. Rectangles are proteins with a t-test *p*-value < 0.01 while the proteins represented by a circle have *p*-value between 0.01 and 0.05.

“for TOC only”

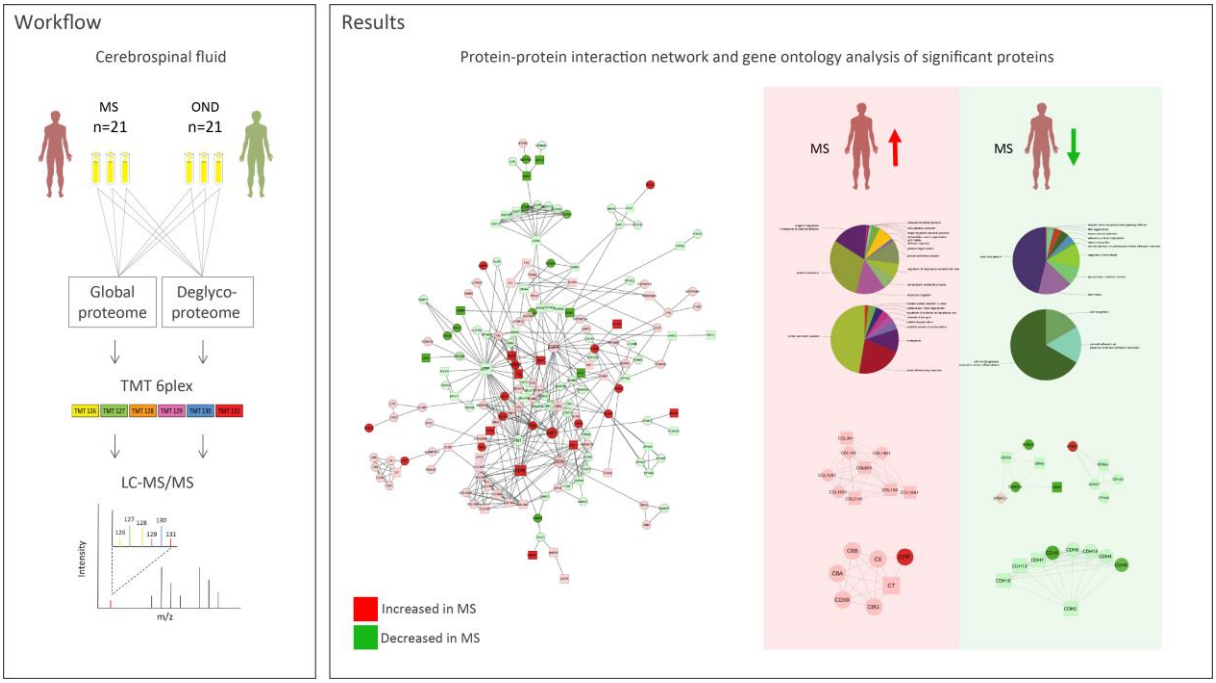
Workflow
Cerebrospinal fluid
MS
n=21
OND
n=21
Global proteome
Deglyco-proteome
TMT 6plex
LC-MS/MS
Intensity
m/z
Results
Protein-protein interaction network and gene ontology analysis of significant proteins
Increased in MS
Decreased in MS
MS
MS